

# Experimental Validation of Crystal Plasticity Models

SAND2013-10485C

**Jay D. Carroll**<sup>1</sup>

**Hojun Lim**<sup>2</sup>

**Brad L. Boyce**<sup>1</sup>

**Corbett C. Battaile**<sup>1</sup>

**Thomas E. Buchheit**<sup>1</sup>

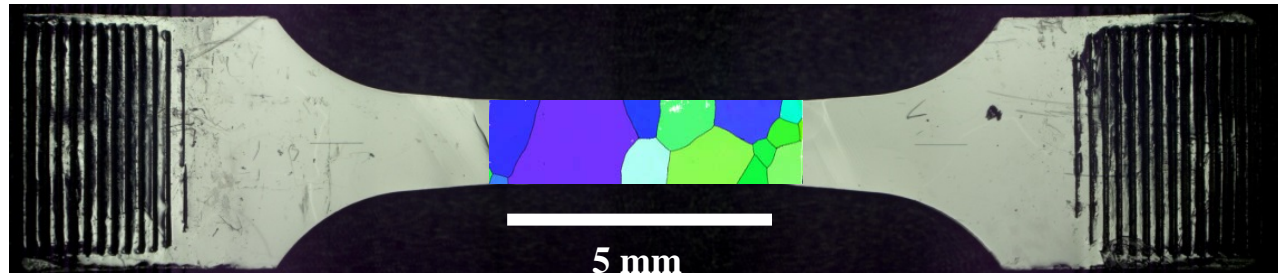
**Christopher R. Weinberger**<sup>3</sup>

<sup>1</sup>**Sandia National Laboratories**, Metallurgy & Materials Joining

<sup>2</sup>**Sandia National Laboratories**, Computational Materials & Data Science

<sup>3</sup>**Drexel University**, Department of Mechanical Engineering & Mechanics

**International Symposium on Plasticity**  
**1/3/2014**



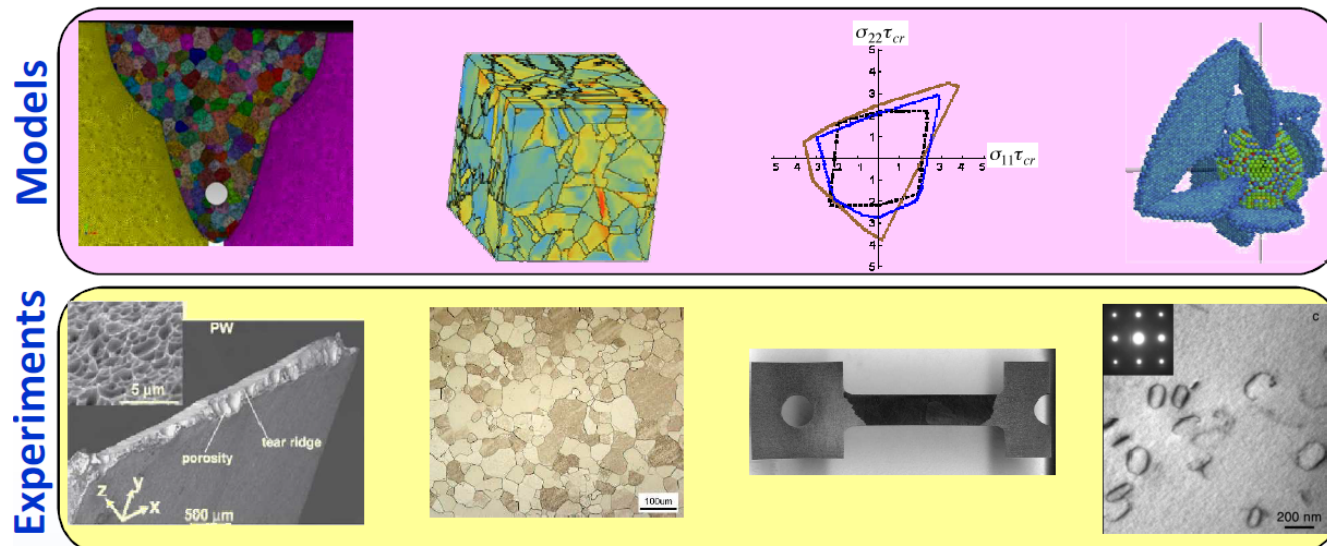
Sandia National Laboratories is a multi-program laboratory managed and operated by Sandia Corporation, a wholly owned subsidiary of Lockheed Martin Corporation, for the U.S. Department of Energy's National Nuclear Security Administration under contract DE-AC04-94AL85000.

- 1. Background**
- 2. Experimental setup**
- 3. Model details**
- 4. Model validation- strain fields**
- 5. Model validation- crystal rotations**
- 6. Conclusions**

- 1. Background**
- 2. Experimental setup**
- 3. Model details**
- 4. Model validation- strain fields**
- 5. Model validation- crystal rotations**
- 6. Conclusions**

# Relate variability in structural behavior to microstructural variability

- Task 4: Modeling Processing Effects on Microstructure
- Task 3: Predict macroscale variability from microstructural statistical models.
- **Task 2: Microscale effects on deformation behavior.**
- Task 1: Atomic/nanoscale defects and dislocation effects.



Material performance  
 $10^0 \text{ m } 10^6 \text{ s}$

Microstructural effects  
 $10^{-3} \text{ m } 10^3 \text{ s}$

Single crystal behavior  
 $10^{-6} \text{ m } 10^0 \text{ s}$

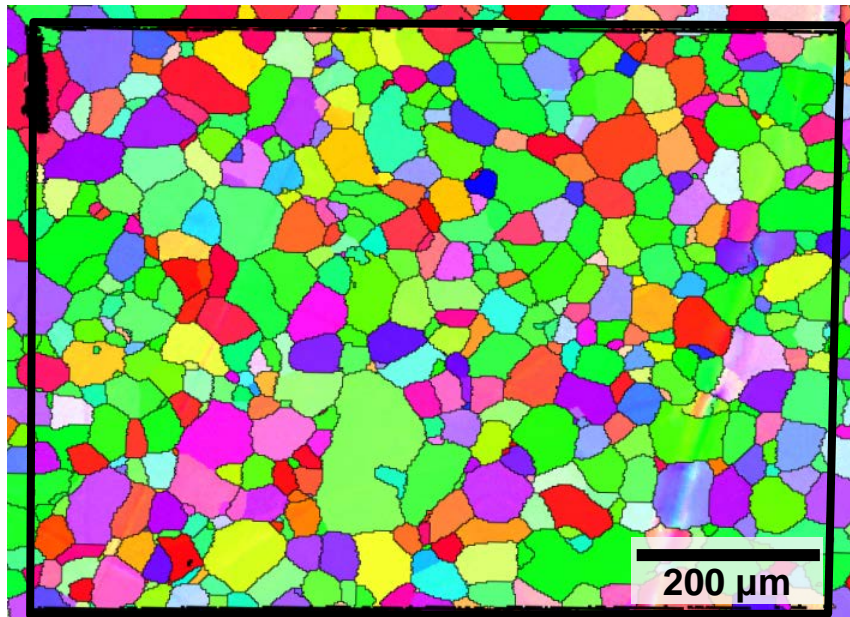
Atomic scale phenomena  
 $10^{-9} \text{ m } 10^{-9} \text{ s}$

Atoms-up: Develop physics-based models to provide scientific insight

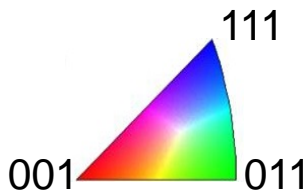
Continuum-down: Augment engineering-scale models to provide customer value

# Local microstructure has significant effects on local deformation.

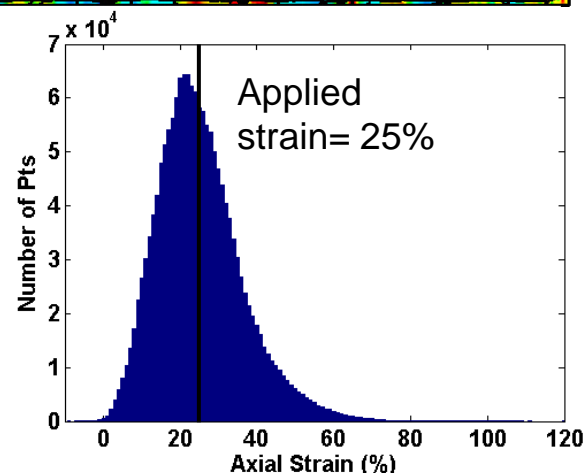
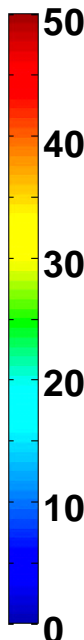
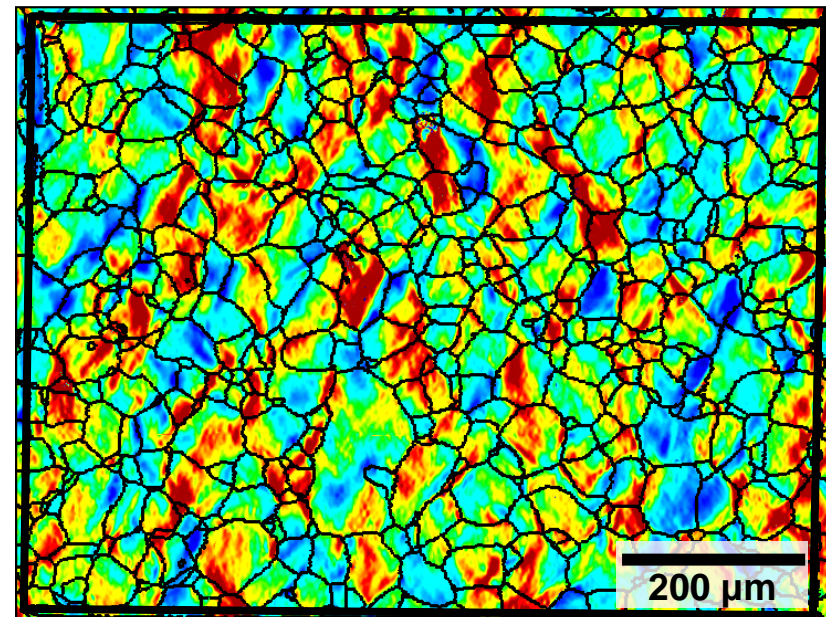
Microstructure (EBSD)



$\xrightarrow{x}$



Effective Strain (%) (DIC)

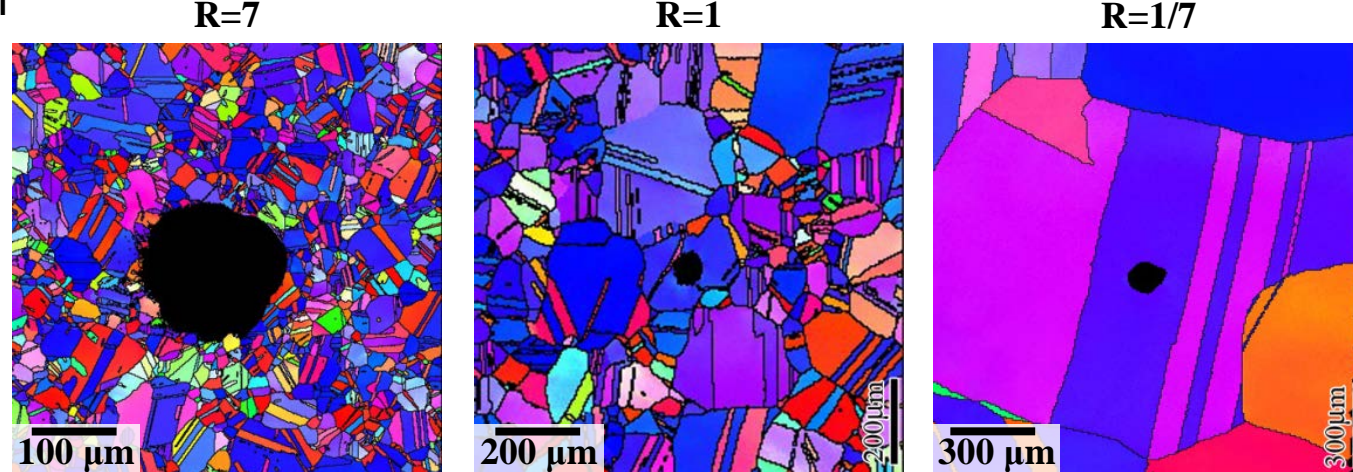


# For small features, microstructure can be more important than the stress concentrator.

- **Experimental measurements**

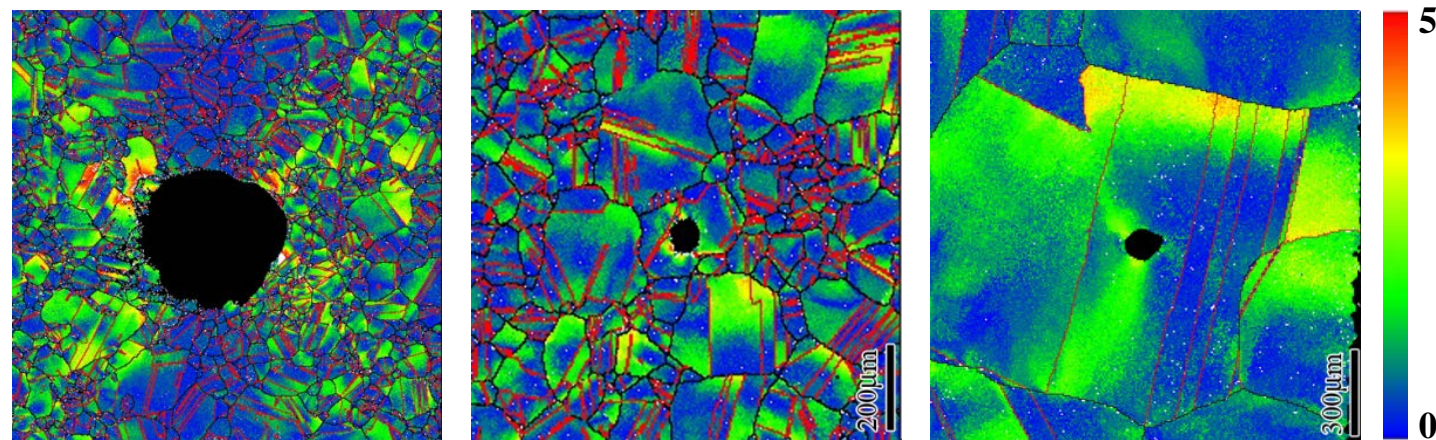
Orientation

↑  
Tensile  
Axis  
↓



$$R = \frac{\text{Hole Size}}{\text{Grain Size}}$$

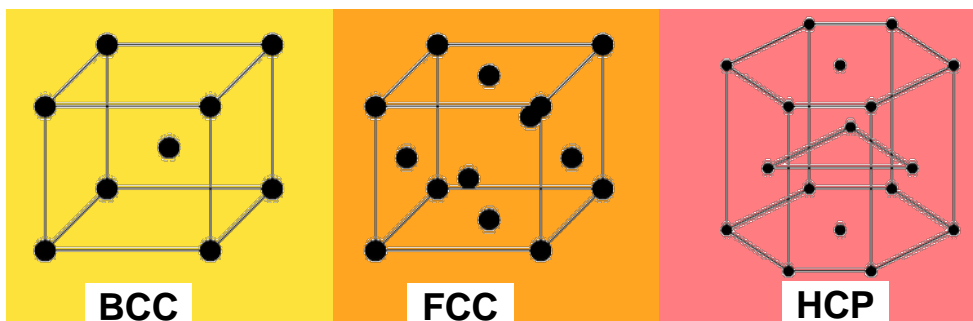
Misorientation  
(≈strain)



**Several important structural metals are BCC.**

7

H	Periodic Table of Density																		He
453.69 Li bcc	1560 Be hcp																		
370.87 Na bcc	923 Mg hcp																		
		HCP	BCC																
336.53 K bcc	1115 Ca fcc	1814 Sc hcp	1941 Ti hcp	2183 V	2180 Cr bcc	1519 Mn	1811 Fe bcc	1768 Co hcp	1728 Ni fcc	1357.8 Cu fcc	692.68 Zn hcp	301.91 Ga							
312.46 Rb bcc	1050 Sr fcc	1799 Y	2128 Zr hcp	2750 Nb bcc	2896 Mo bcc	2430 Tc hcp	2607 Ru hcp	2237 Rh fcc	1828 Pd fcc	1235 Ag fcc	594 Cd	430 In	505 Sn	904 Sb					
301.59 Cs bcc	1000 Ba bcc	*	2506 Hf hcp	3290 Ta bcc	3422 W bcc	3186 Re hcp	3306 Os hcp	2446 Ir fcc	1768 Pt fcc	1337.33 Au fcc	234.32 Hg	577 Tl hcp	600.61 Pb fcc	544.7 Bi	527 Po				
Fr	973 Ra bcc	**	Rf	Db	Sg	Bh	Hs	Mt	Ds	Rg	Cn	Uut	Fl	Uup	Lv	Uus	Uuo		
*		1193 La dhcp	1068 Ce fcc	1208 Pr dhcp	1297 Nd dhcp	1315 Pm dhcp	1345 Sm	1099 Eu bcc	1585 Gd hcp	1629 Tb hcp	1680 Dy hcp	1734 Ho hcp	1802 Er hcp	1818 Tm hcp	1097 Yb fcc	1925 Lu hcp			
**		1323 Ac fcc	2115 Th fcc	1841 Pa	1405.3 U	917 Np	912.5 Pu	1449 Am dhcp	1613 Cm dhcp	1323 Bk dhcp	1173 Cf dhcp	1133 Es fcc	Fm	Md	No	Lr			



The top number in the cell is the melting point (in K)

 **dhcp**: double hexagonal close packed

## unusual structure

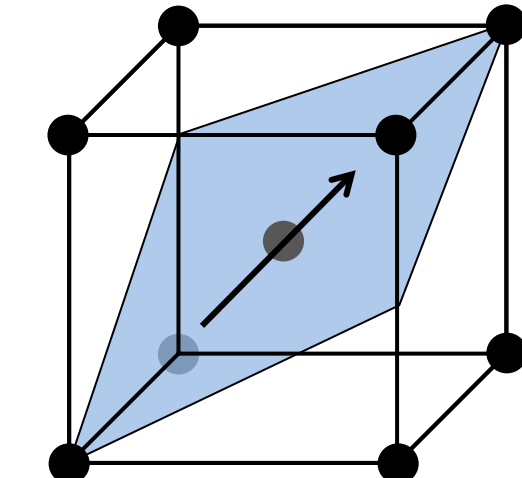
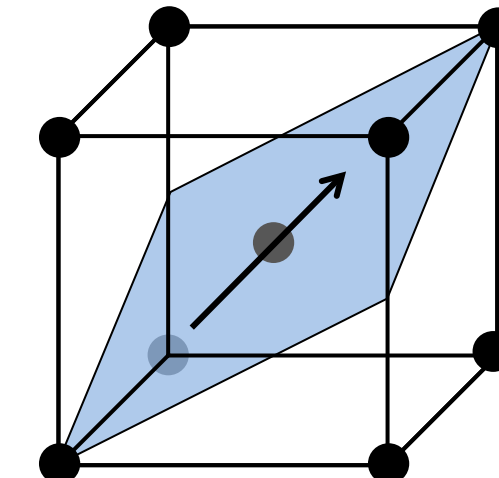
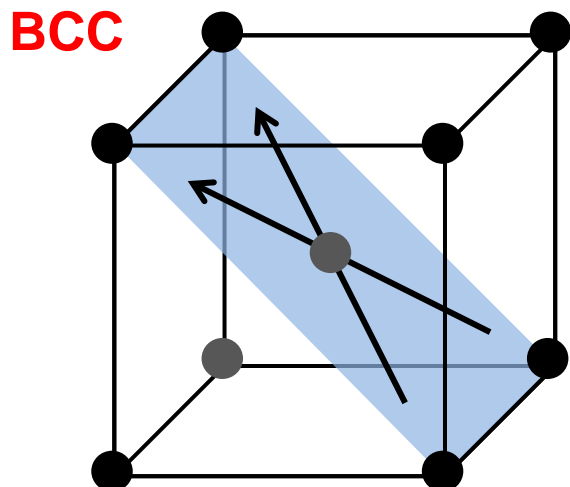
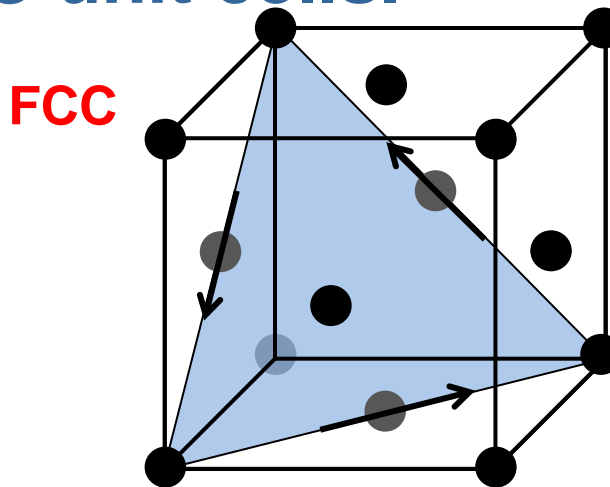
## nonmeta

unknown or uncertain



# Images showing slip planes and directions in FCC and BCC unit cells.

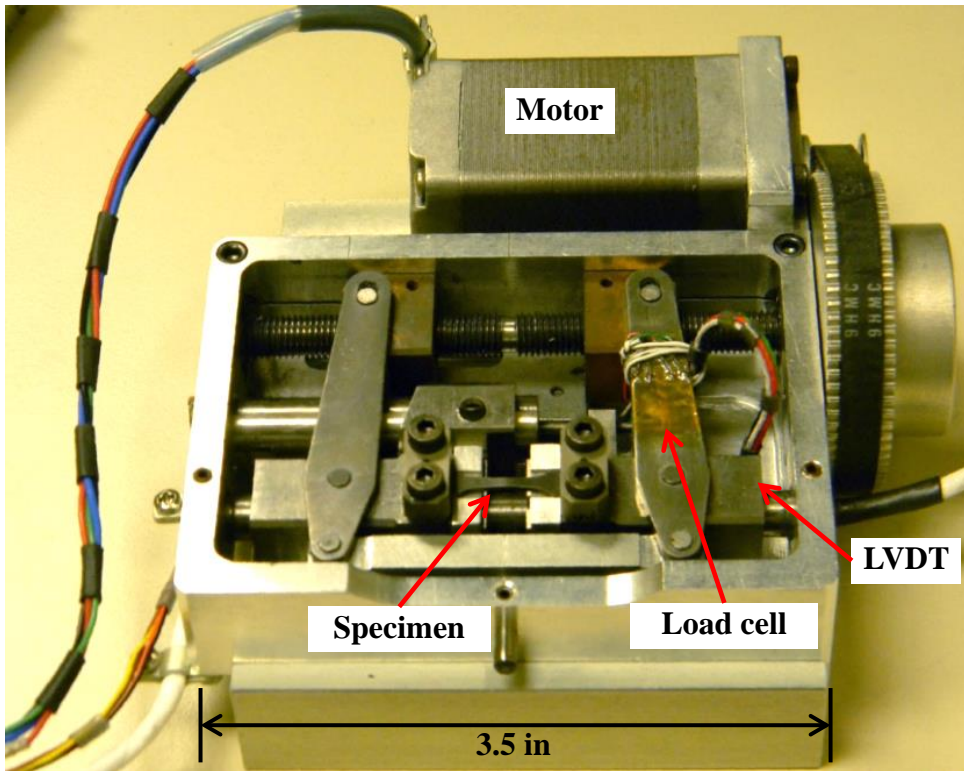
8



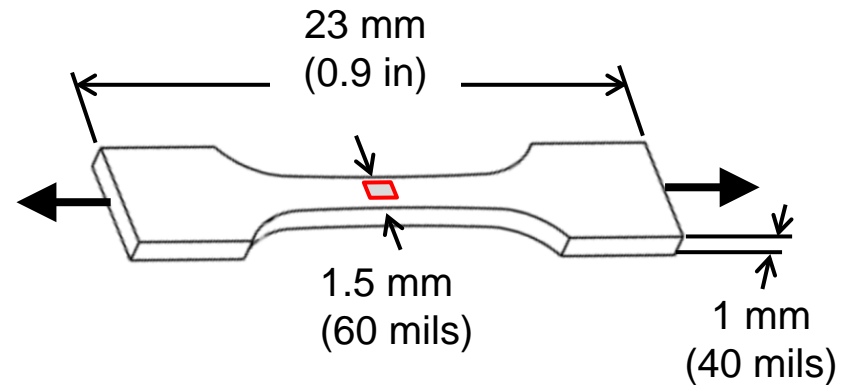
1. **Background**
2. **Experimental setup**
3. **Model details**
4. **Model validation- strain fields**
5. **Model validation- crystal rotations**
6. **Conclusions**

# An in situ load frame developed at Sandia allows loading inside the SEM.

10

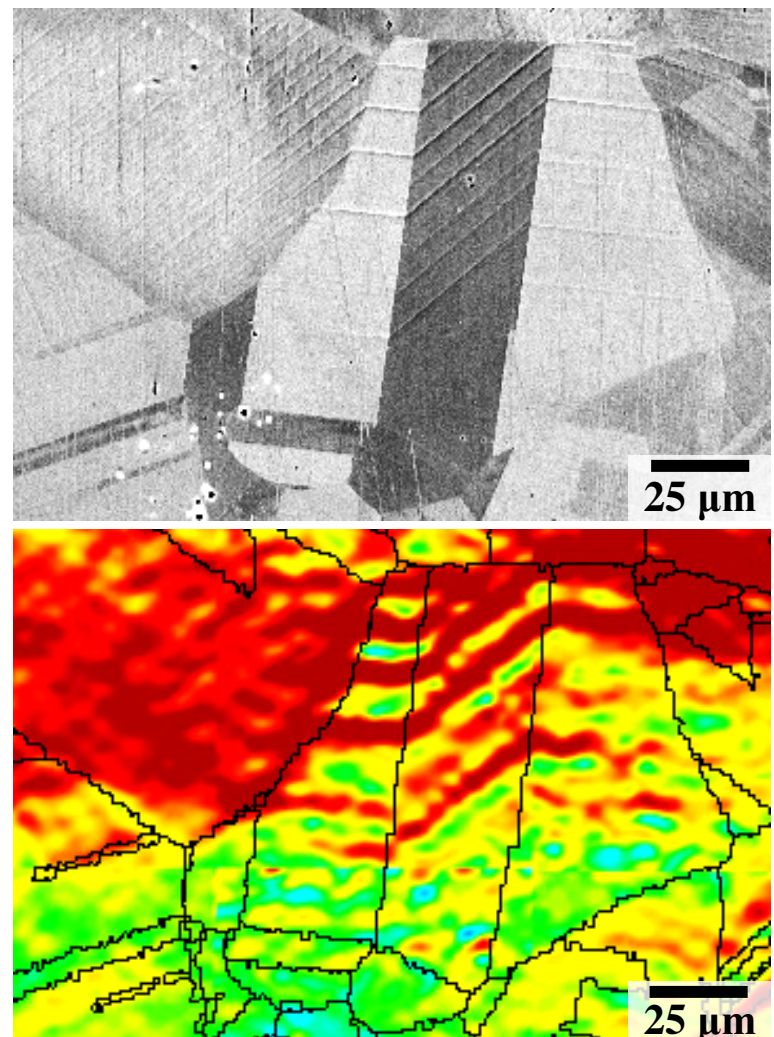
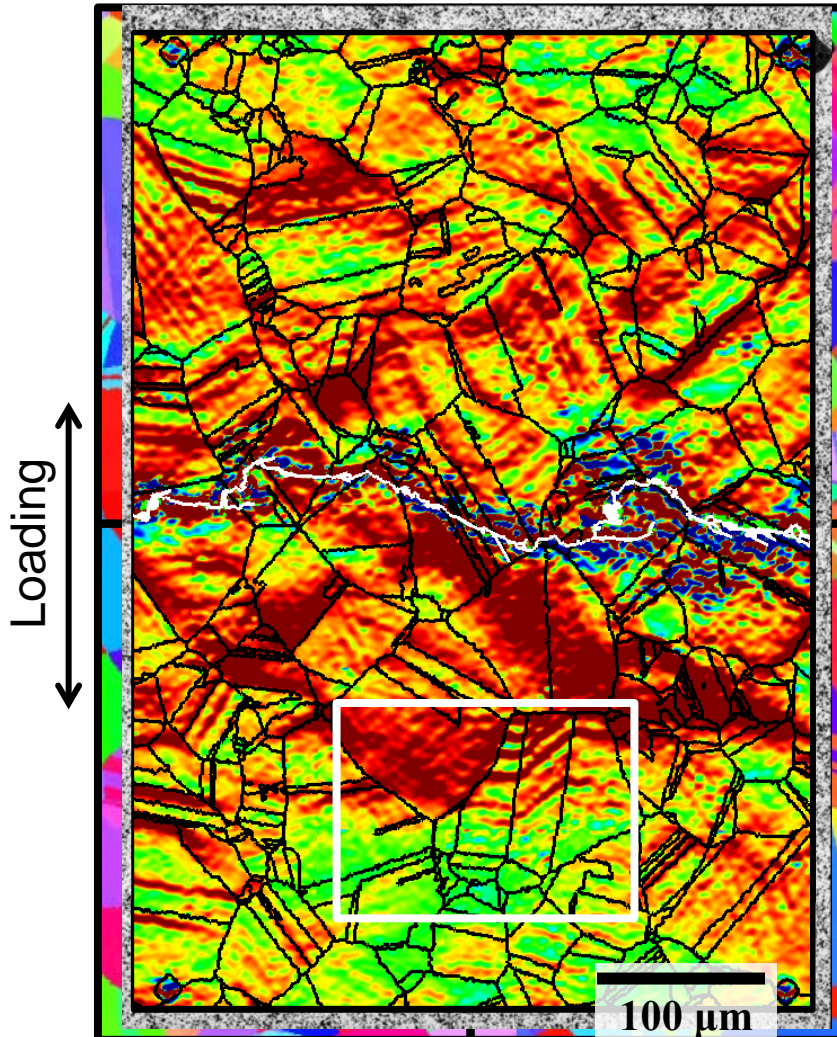


- Can make DIC and EBSD measurements at load.



Tapered gage section is narrower at center.

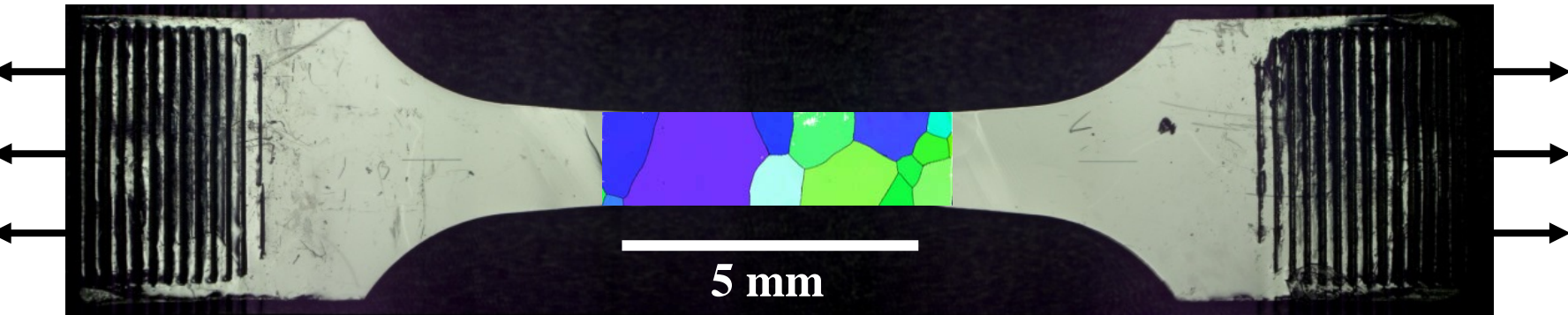
# Our high resolution experimental technique relates subgrain level strains to microstructure.



- Carroll JD, Abuzaid W, Lambros J, Sehitoglu H, *Int. J. Fatigue*, v. 57 (2013).
- Carroll JD, Abuzaid W, Lambros J, Sehitoglu H, *Int J. Fracture*, v. 180 (2012).
- Carroll JD, Abuzaid W, Lambros J, Sehitoglu H, *Rev. Sci Inst.*, v. 81 (2010).

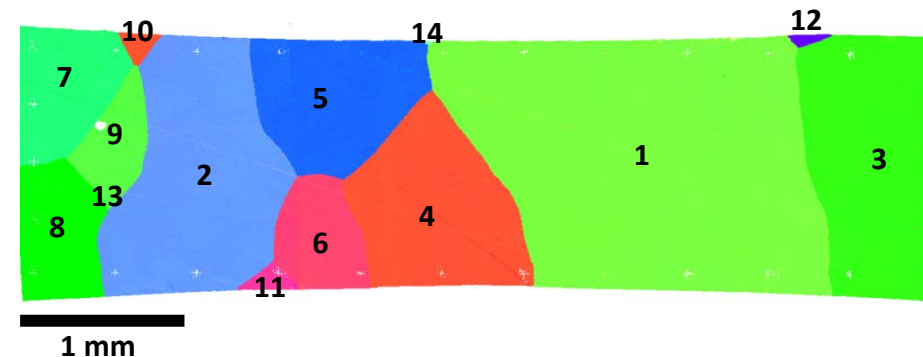
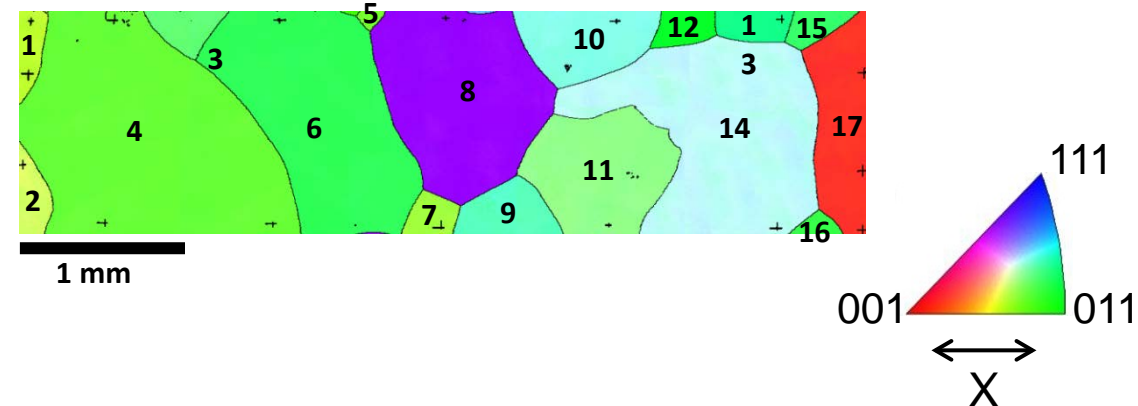
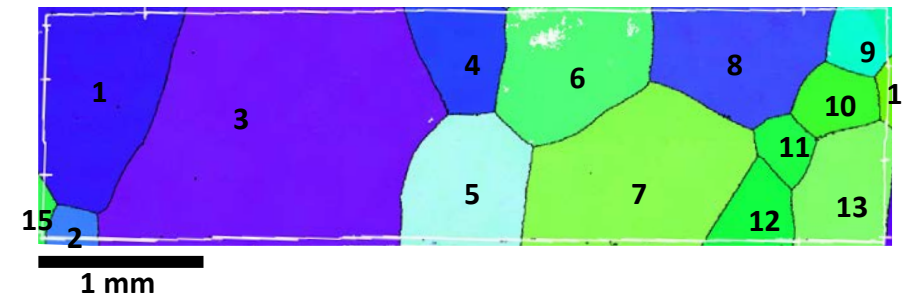
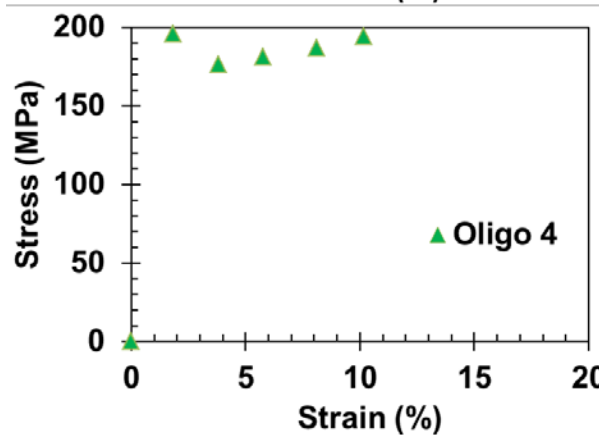
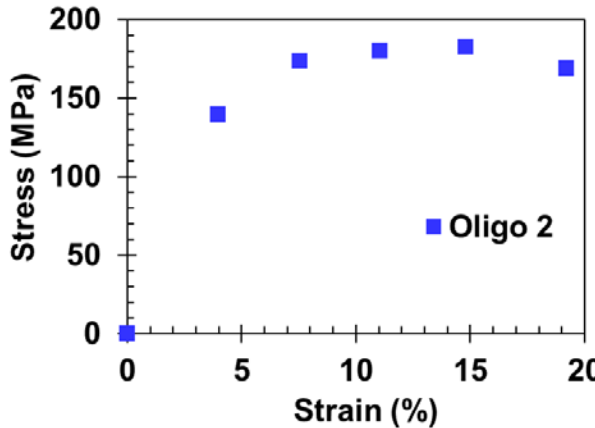
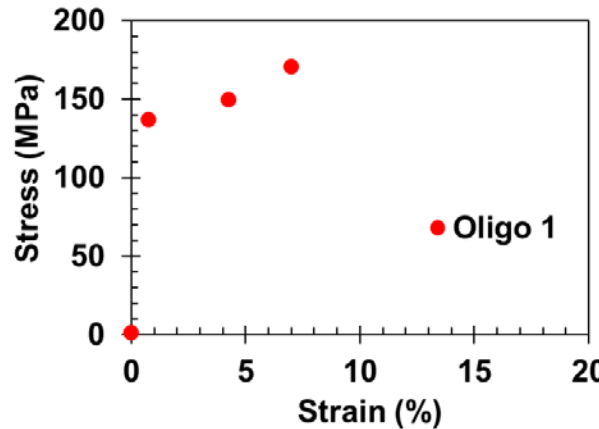
# Oligocrystals

Specimens where deformation is controlled by a few grains (3–20).



- Ta oligocrystals were made by annealing.
- Mostly columnar, 2D grain structure.

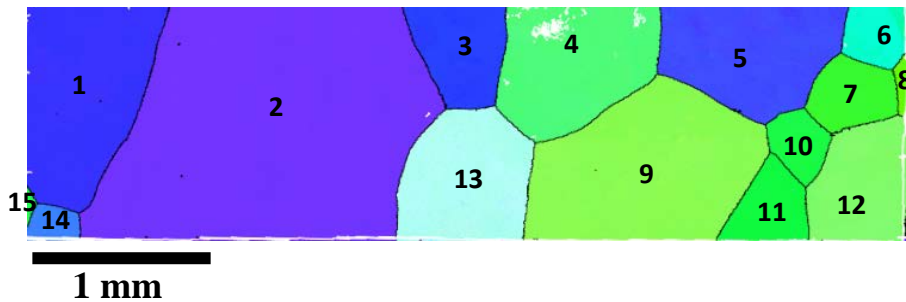
# Loaded three oligocrystal specimens



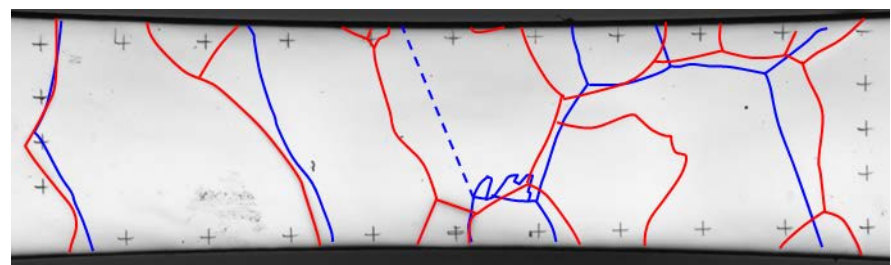
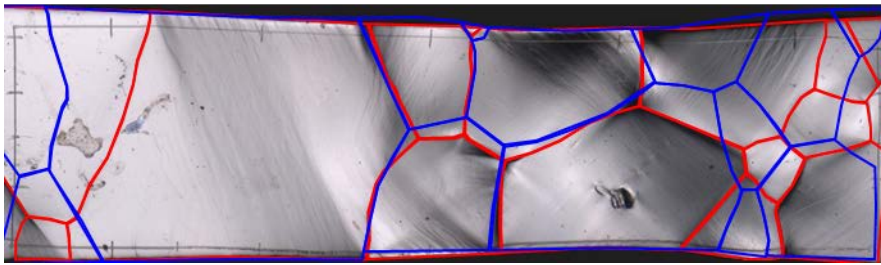
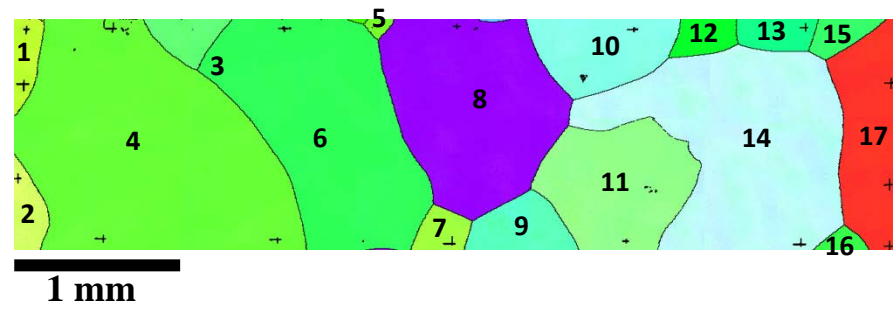
# Grain structure in specimens is pseudo-2D. Most grains are nearly columnar.

14

Oligo 1



Oligo 2



— Grain boundary (Front) — Grain boundary (Back)

1. **Background**
2. **Experimental setup**
3. **Model details**
4. **Model validation- strain fields**
5. **Model validation- crystal rotations**
6. **Conclusions**

# Crystal Plasticity Model Equations

- 24 {110}<111> slip systems

- **Slip rate:**  $\dot{\gamma}^\alpha = \dot{\gamma}_0^\alpha \left( \frac{\tau^\alpha}{g^\alpha} \right)^{1/m}$  (Hutchinson, 1976)

- **Slip resistance:**  $g^\alpha = \min\left(\tau_{EI}^{*\alpha}, \tau_{LT}^{*\alpha}\right) + \tau_{obs}^\alpha$ 

$\tau_{EI}^{*\alpha}$   
 $\tau_{LT}^{*\alpha}$

$\longrightarrow$

Obstacle stress

$\tau_{obs}^\alpha$

$\longrightarrow$

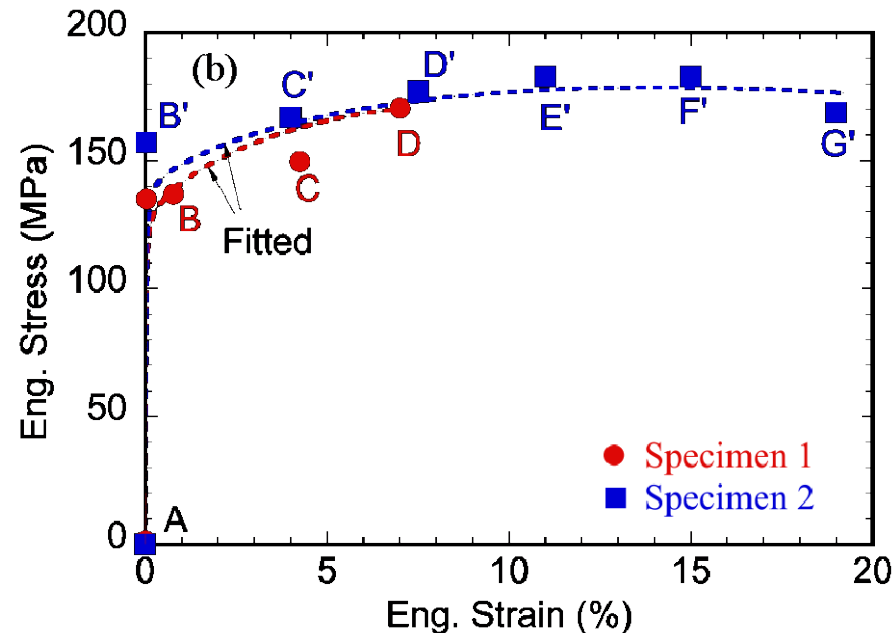
Lattice friction

- **Obstacle stress:**  $\tau_{obs}^\alpha = A\mu b \sqrt{\sum_{\beta=1}^{NS} \rho^\beta}$  (Taylor, 1934)

$$\dot{\rho}^\alpha = \left( \kappa_1 \sqrt{\sum_{\beta=1}^{NS} \rho^\beta} - \kappa_2 \rho^\alpha \right) \cdot |\dot{\gamma}^\alpha| \quad (\text{Kocks, 1976})$$

For more model details, see Lim et al. "Temperature and Strain Rate Effects on the Dislocation Plasticity of BCC Transition Metals" in room xx at time xx.

# Crystal plasticity finite element model.



## Slip Rate

Obstacle Strength		Lattice Resistance		Elastic Coefficients		Obstacle Strength	
Parameters	Values	Parameters	Values	Parameters	Values	Parameters	Values
$m$	0.012	$\tau_0^{LT}$	406 MPa	$C_{11}$	267 GPa	$\kappa_1$	$1.4 \times 10^6 \text{ m}^{-1}$
$\dot{\gamma}_0$	$0.001 \text{ s}^{-1}$	$\tau_0^{EI}$	320 MPa	$C_{12}$	161 GPa	$\kappa_2$	14
$A$	0.4	$2H_k$	0.85 eV	$C_{44}$	82.5 GPa	$\tau_{\text{obs},0}^1$	27 MPa
$b$	$2.87 \text{ \AA}$	$\dot{\epsilon}_0$	$2.99 \times 10^6 \text{ s}^{-1}$	$\mu$	70.7 GPa	$\tau_{\text{obs},0}^2$	37 MPa

From literature

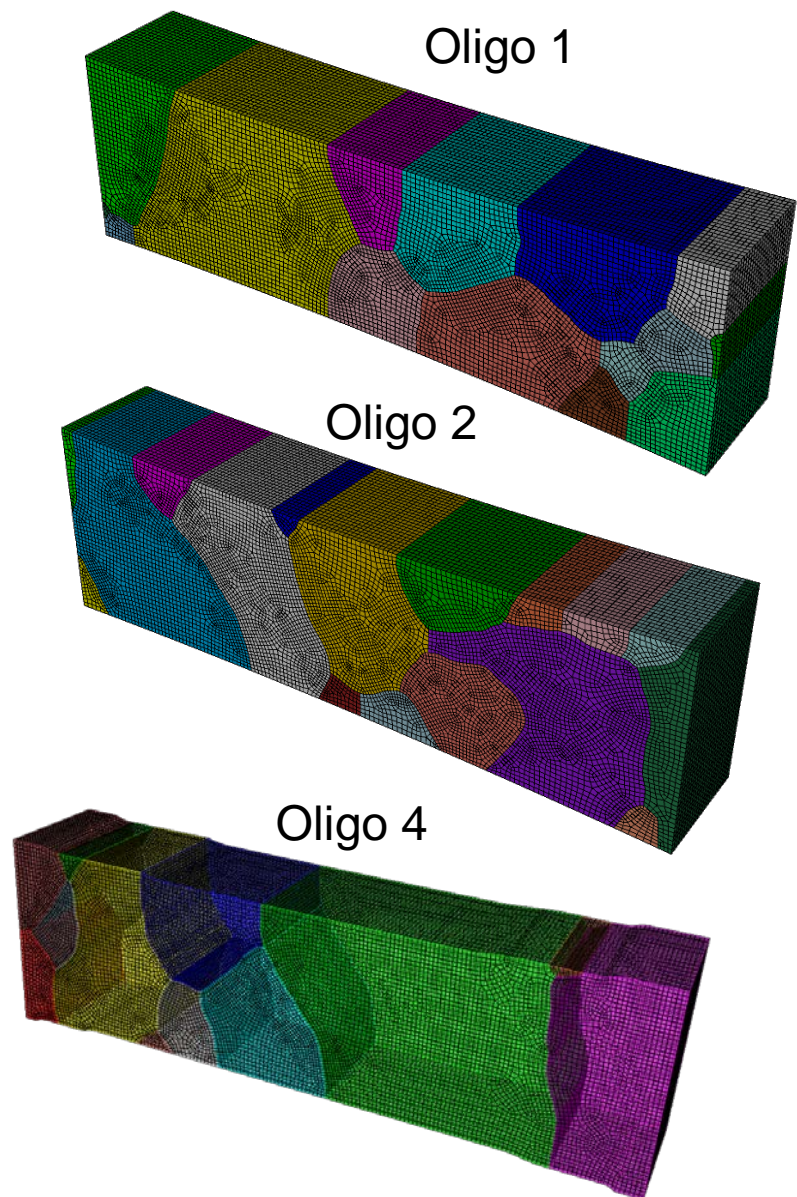
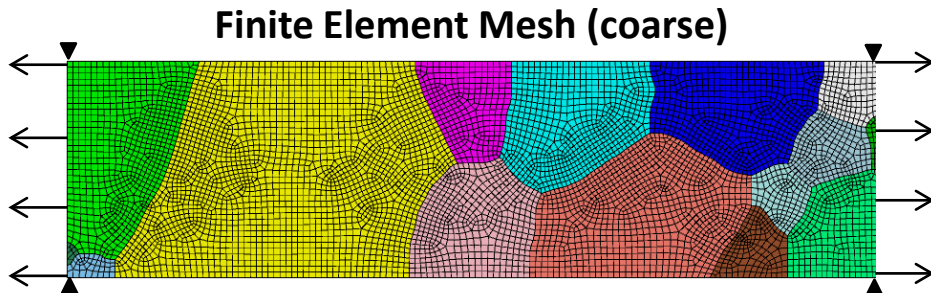
From fits to single crystal experiments

From literature

Fitting stress-strain data for each specimen

# Finite element meshes for each specimen cover most of the gage section with pseudo-3d mesh.

- FEM code (JAS-3D) developed at Sandia.
- Dislocation density based hardening.
- Hexahedral elements (8 nodes).
- One orientation per element.
- 50 elements through specimen thickness.
  - ~1.5 million total elements
  - ~30,000 surface elements



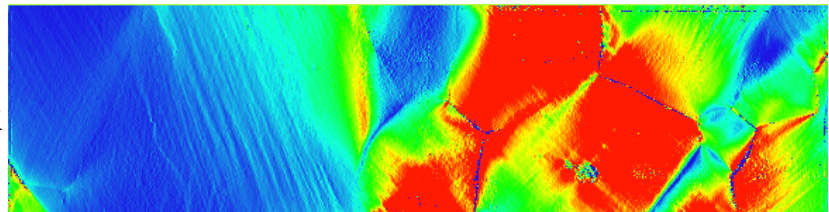
1. **Background**
2. **Experimental setup**
3. **Model details**
4. **Model validation- strain fields**
5. **Model validation- crystal rotations**
6. **Conclusions**

# Oligo 1 Strain fields agree in most places.

20

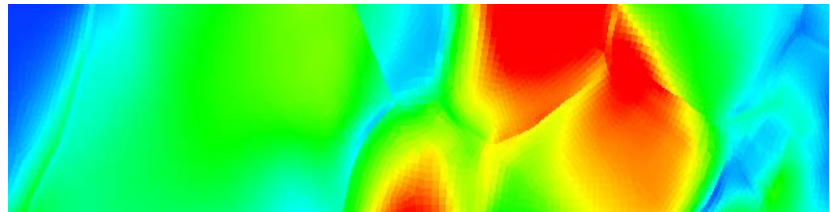
Experimental Strains (DIC)

$\epsilon_{xx}$

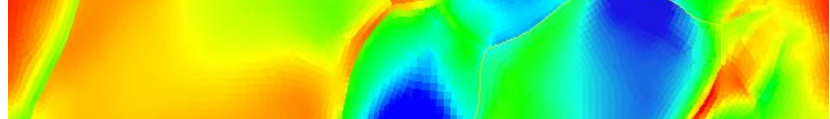


Model Strains (CP-FEM)

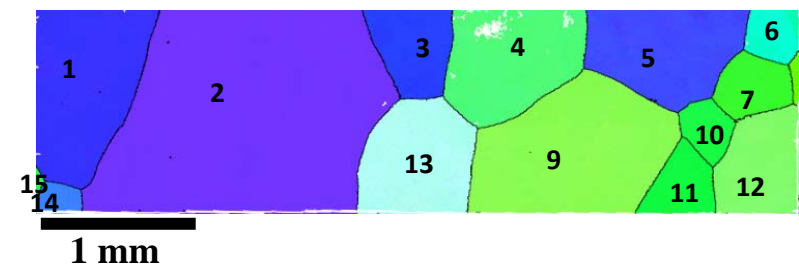
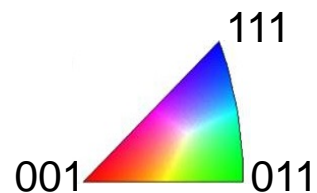
$\epsilon_{yy}$



$\epsilon_{xy}$



Model only considers  
slip on {110} planes.

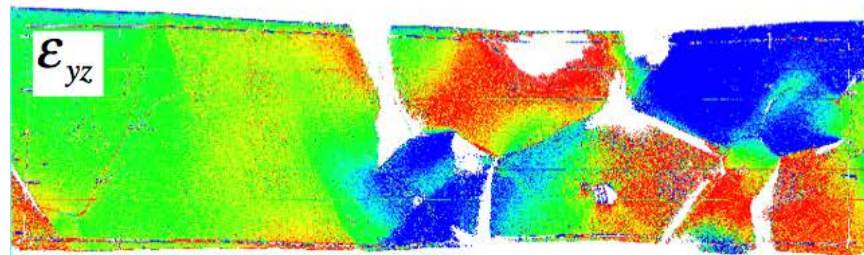
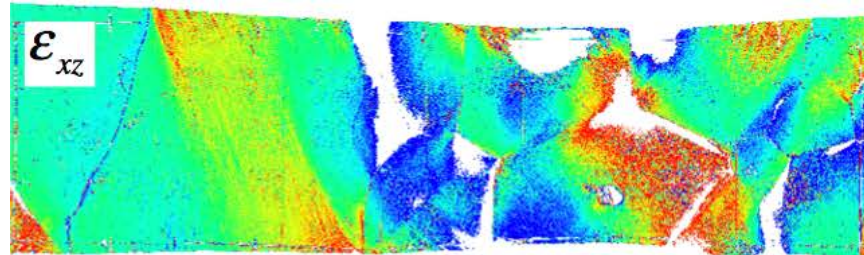


# Out-of-plane strain fields agree within most grains.

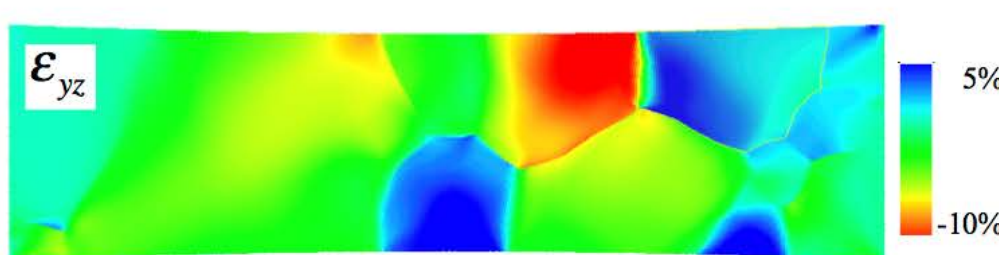
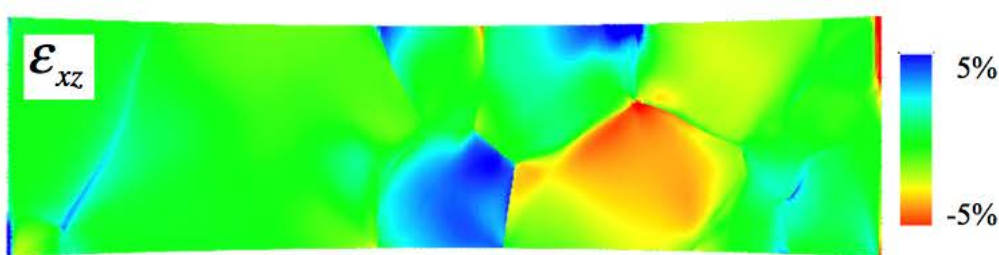
21

## Specimen 1 (6.8% applied strain)

Profilometry Measurements



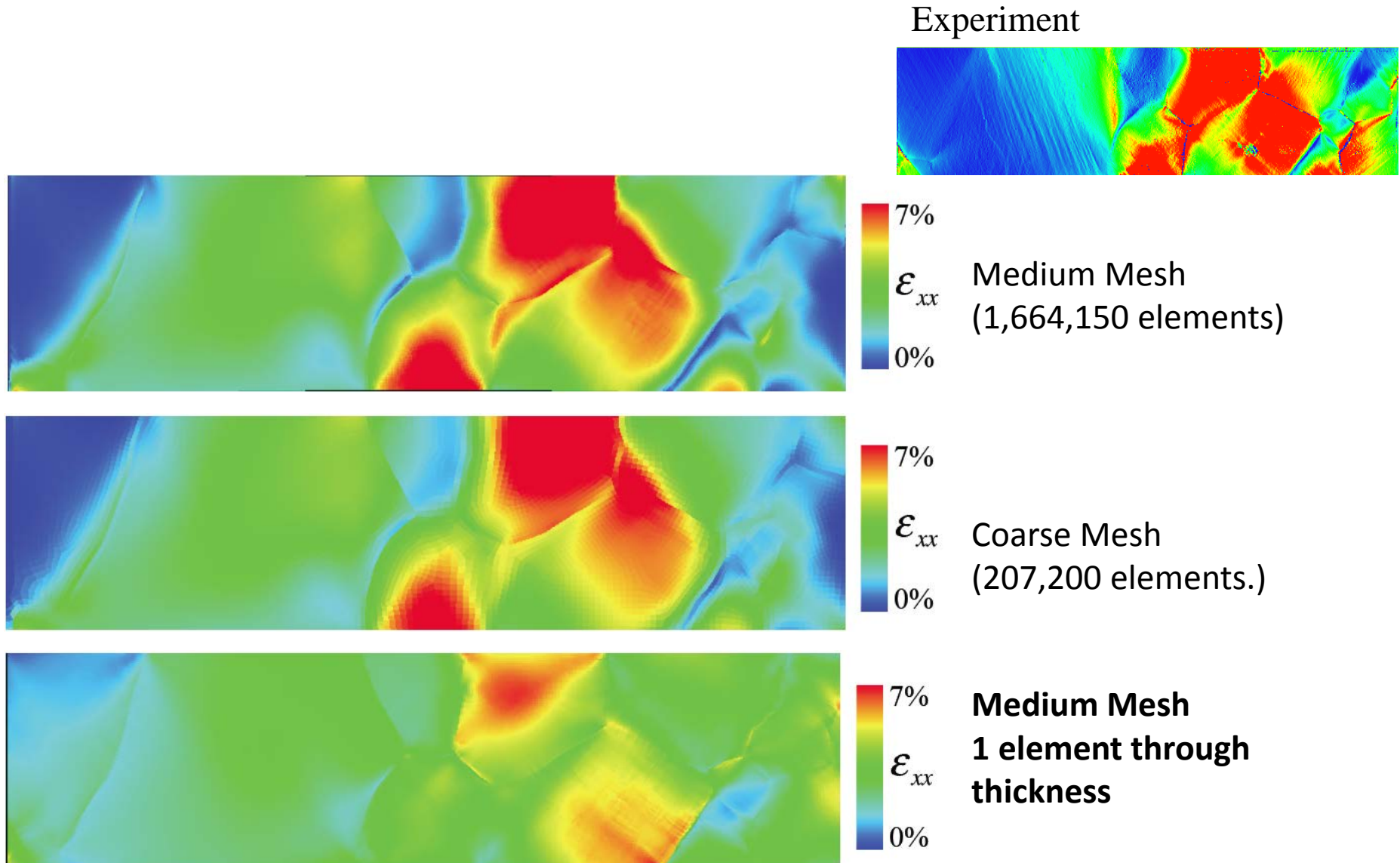
CP-FEM Predictions



- Many grain boundaries have large strains not captured by model.

# Mesh refinement has a slight affect on strain field. Including a pseudo-3d mesh has a significant effect.

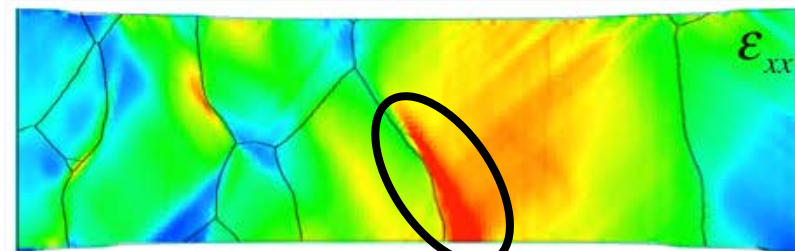
22



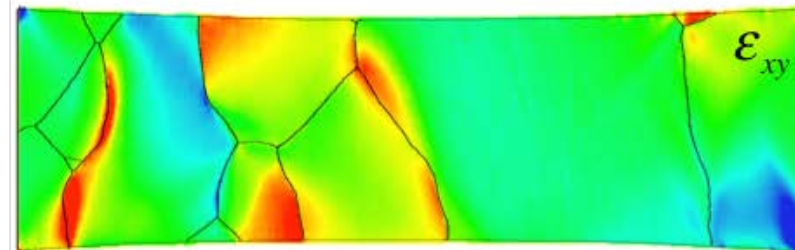
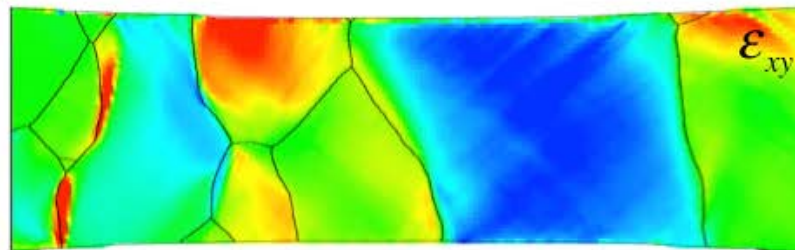
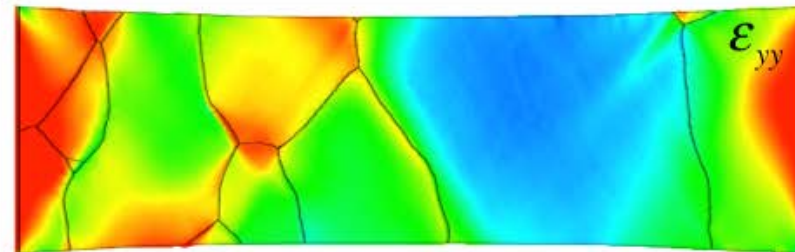
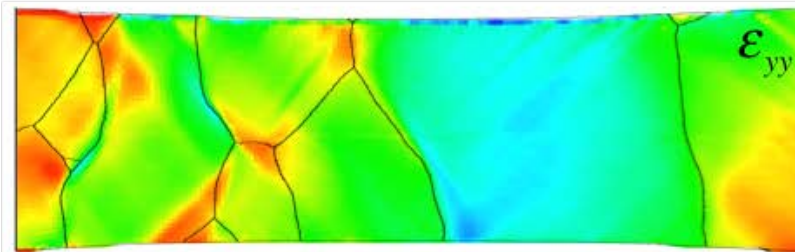
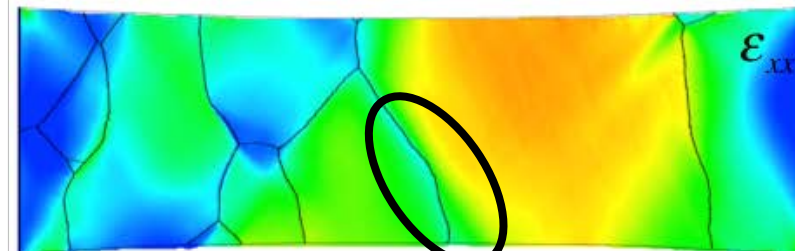
# Oligo 4 Strain fields agree in most places.

23

Experimental Strains (DIC)

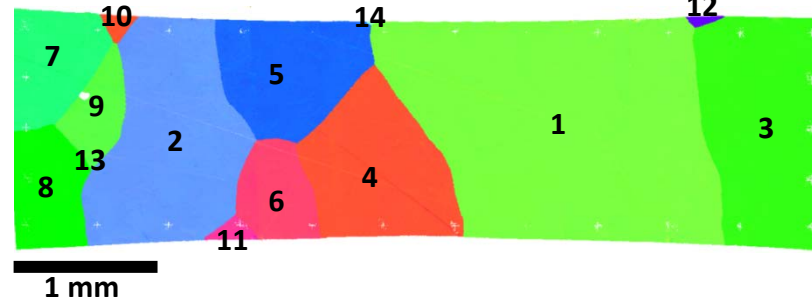
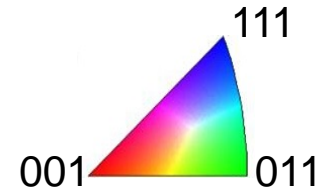


Model Strains (CP-FEM)



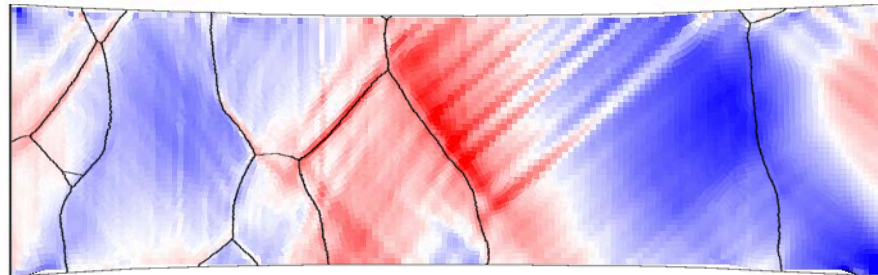
(10% global strain).

Model only considers  
slip on  $\{110\}$  planes.



# Quantitative, pointwise comparison of measured and predicted strains.

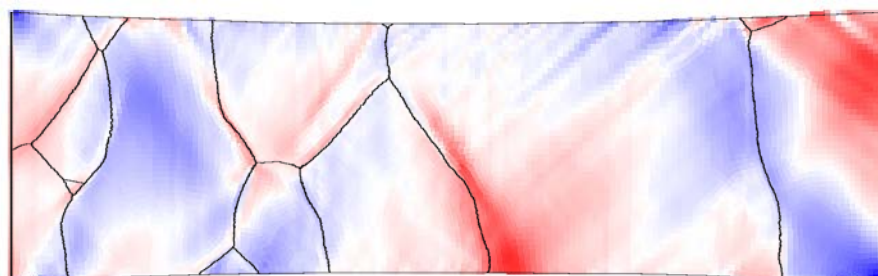
$$\Delta\epsilon = \epsilon_{measured} - \epsilon_{predicted}$$



(a)  $\epsilon = 0.02$  (Point B)



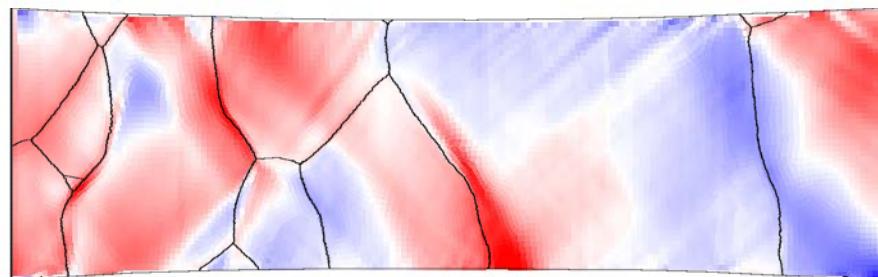
$$\Delta\epsilon_{xx}(\max) = 0.024$$
$$\Delta\epsilon_{xx}(\min) = -0.038$$



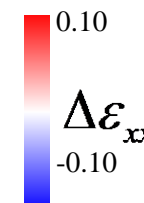
(b)  $\epsilon = 0.06$  (Point D)



$$\Delta\epsilon_{xx}(\max) = 0.052$$
$$\Delta\epsilon_{xx}(\min) = -0.074$$



(c)  $\epsilon = 0.01$  (Point F)

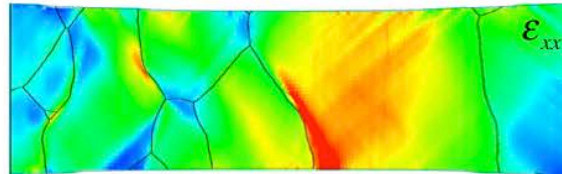


$$\Delta\epsilon_{xx}(\max) = 0.153$$
$$\Delta\epsilon_{xx}(\min) = -0.106$$

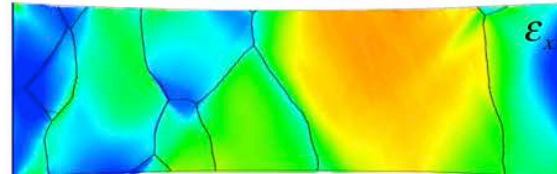
# Oligo 4 Disagreement between measured and predicted strain fields is explained by 3d effects.

25

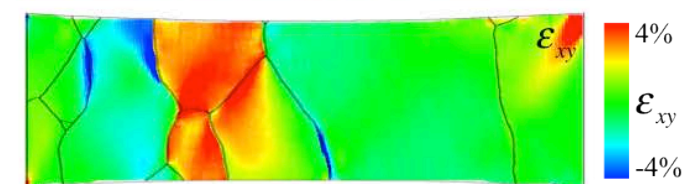
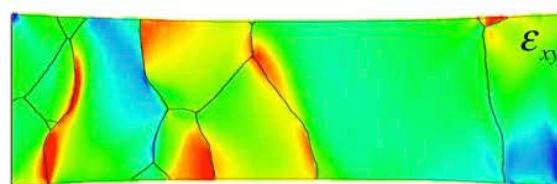
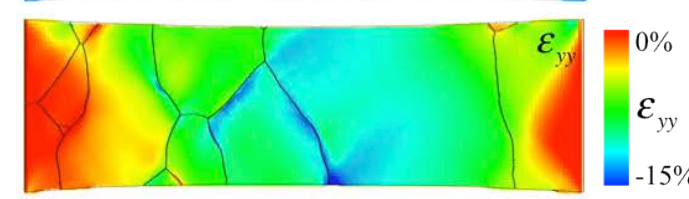
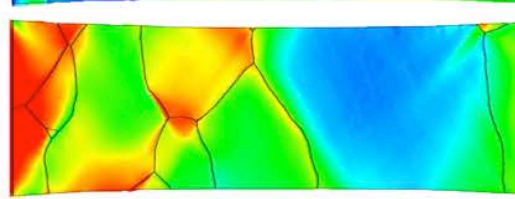
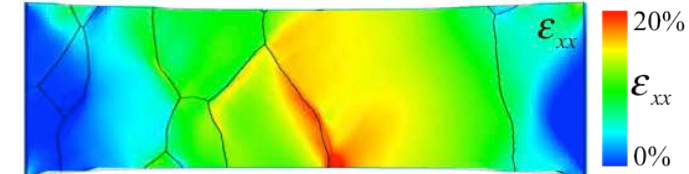
(a) HR-DIC (Front side)



(b) CP-FEM (Front side)

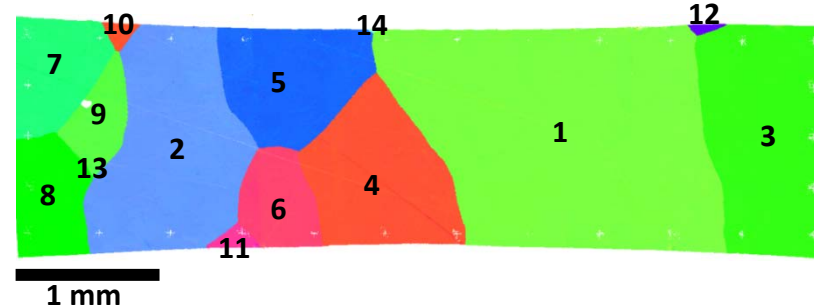
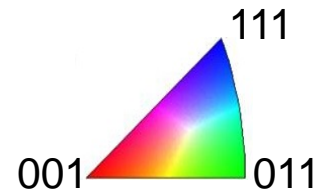


(c) CP-FEM (Back side)



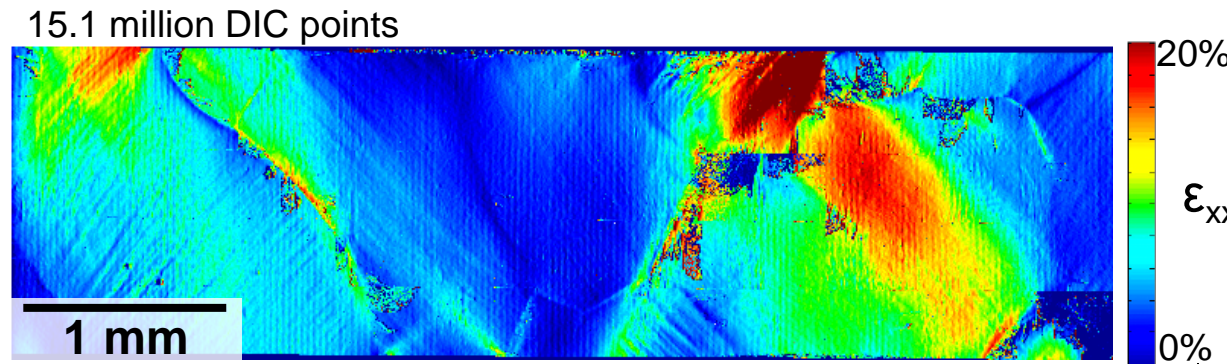
(10% global strain).

Model only considers  
slip on  $\{110\}$  planes.

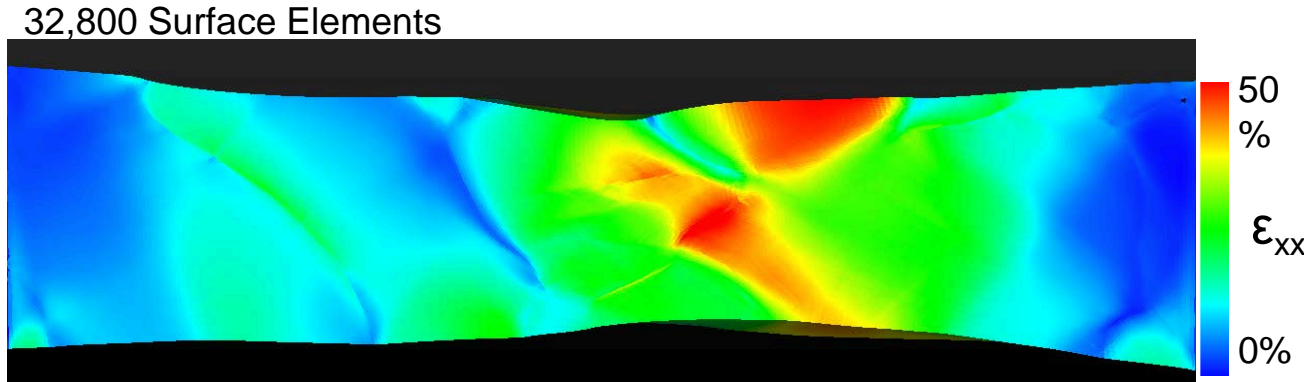


# Oligo 2: Modeling with $\{110\}$ and $\{112\}$ slip planes give different results, but with roughly the same accuracy.

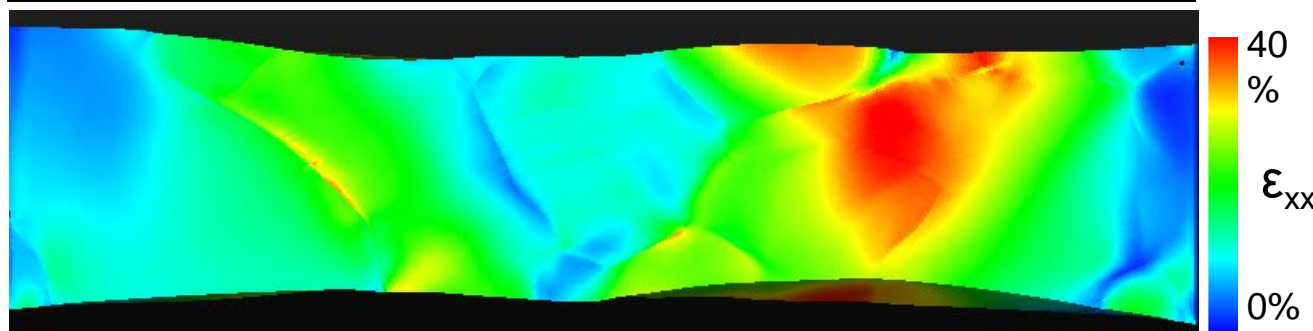
**Experiment**  
DIC  
 $\sim 10\%$   
strain



**Model**  
 $\{110\}$  slip  
 $19\%$   
strain

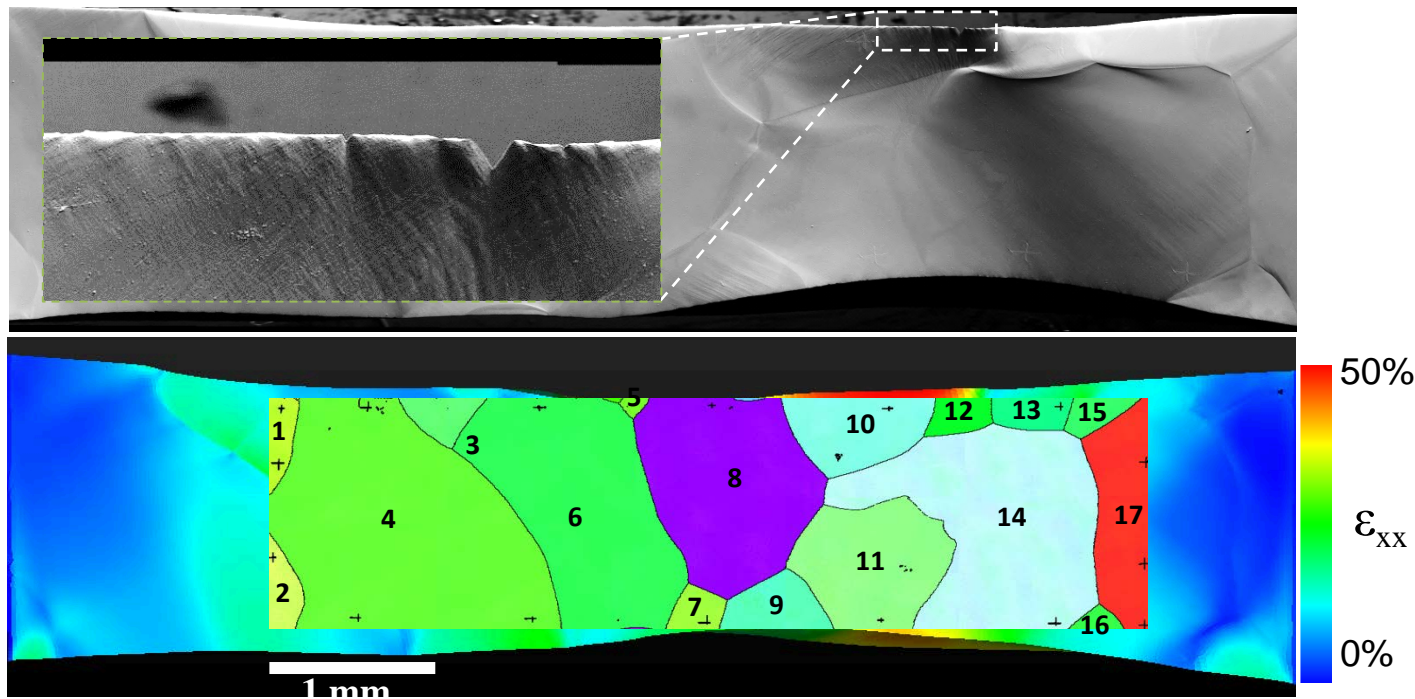
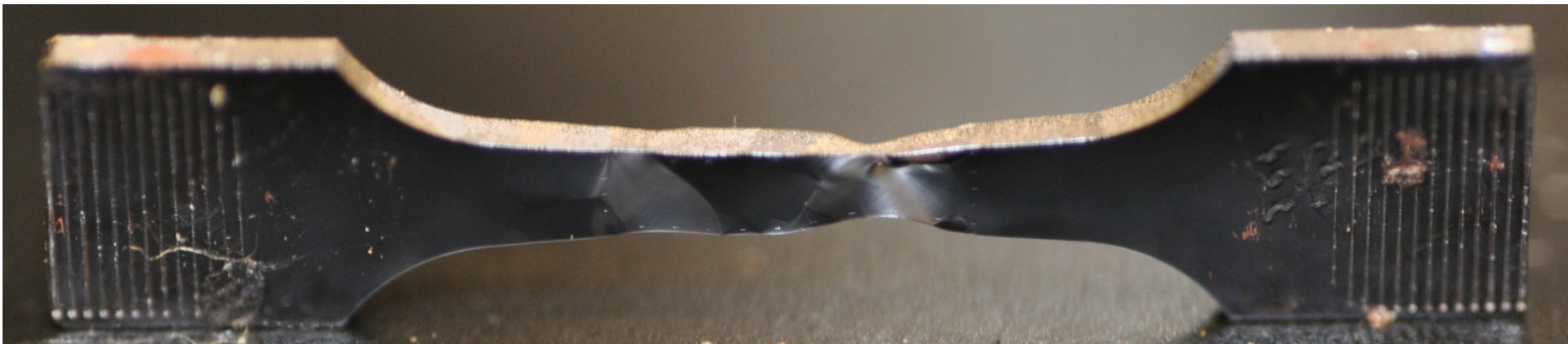


**Model**  
 $\{112\}$  slip  
 $19\%$   
strain



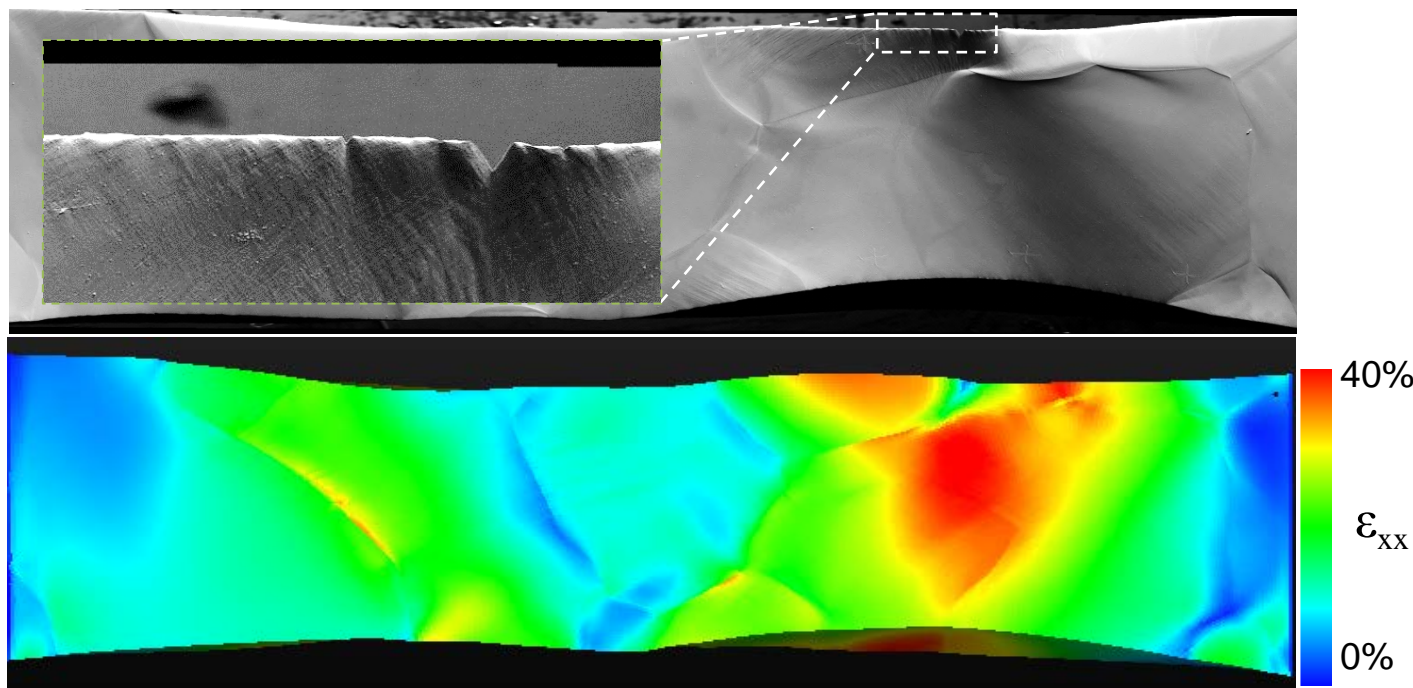
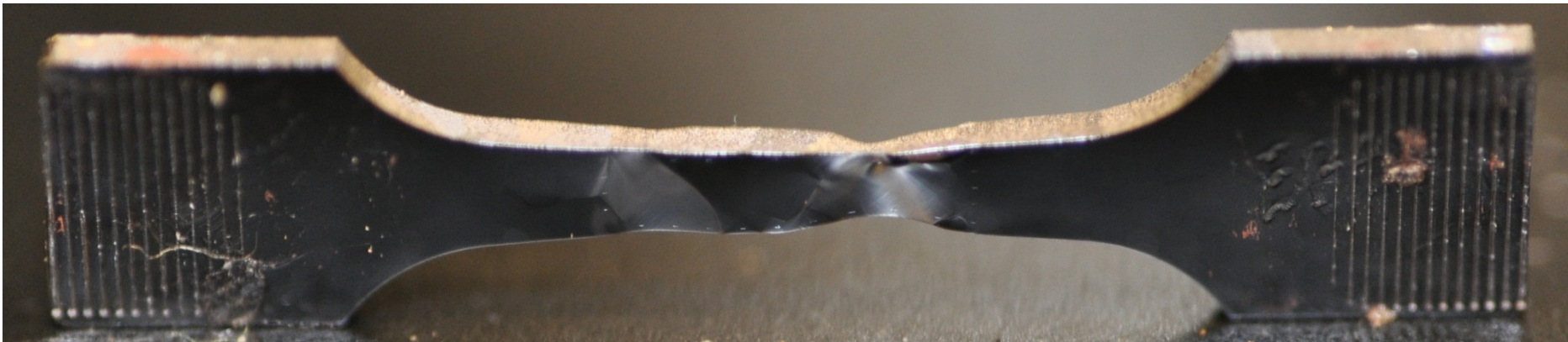
# Model predicts high strain at location of observed crack initiation.

27

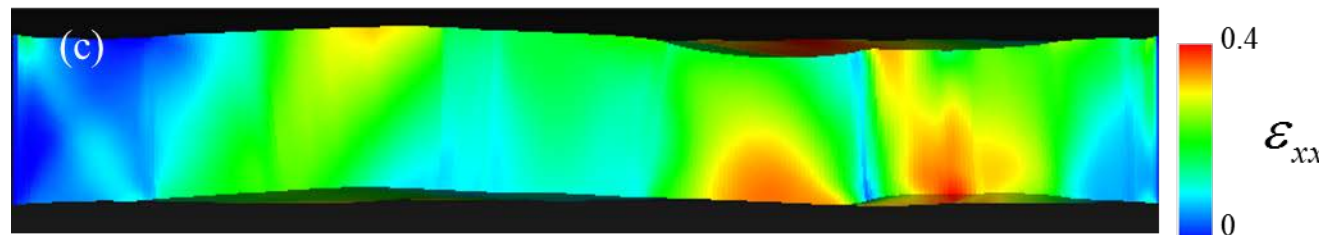
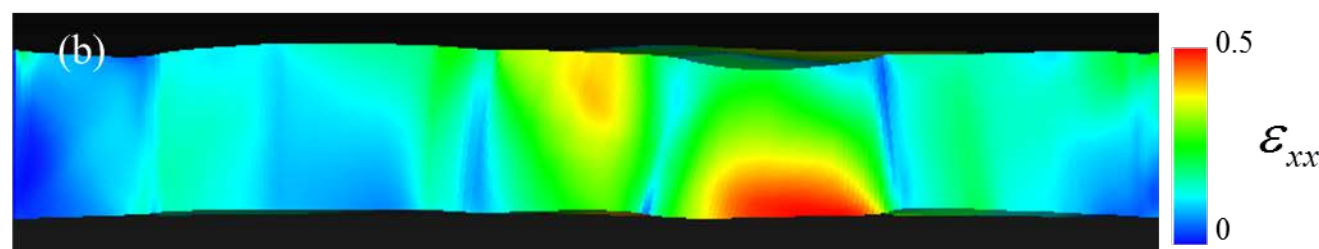
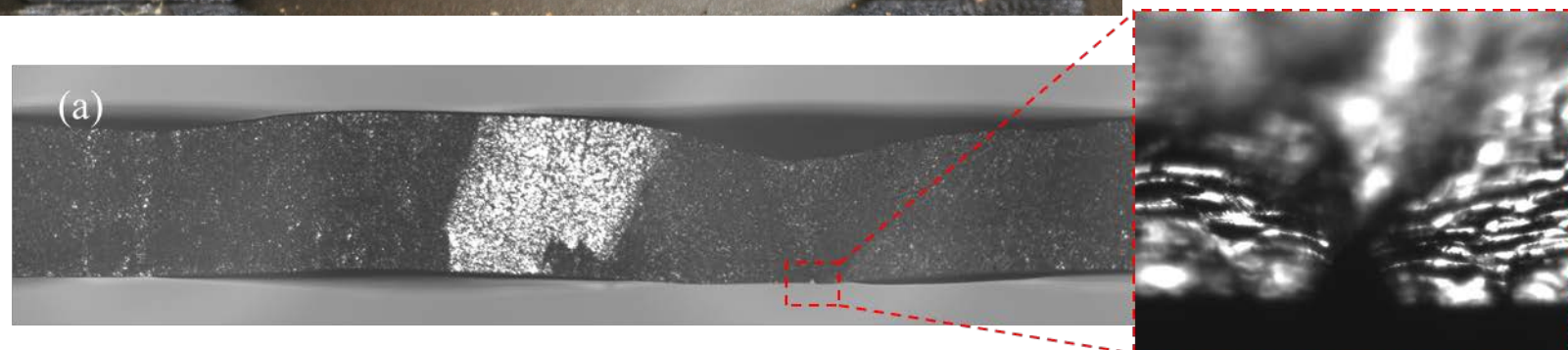


# Model predicts high strain at location of observed crack initiation.

28



# In 3D, model predicts failure initiation on front surface.

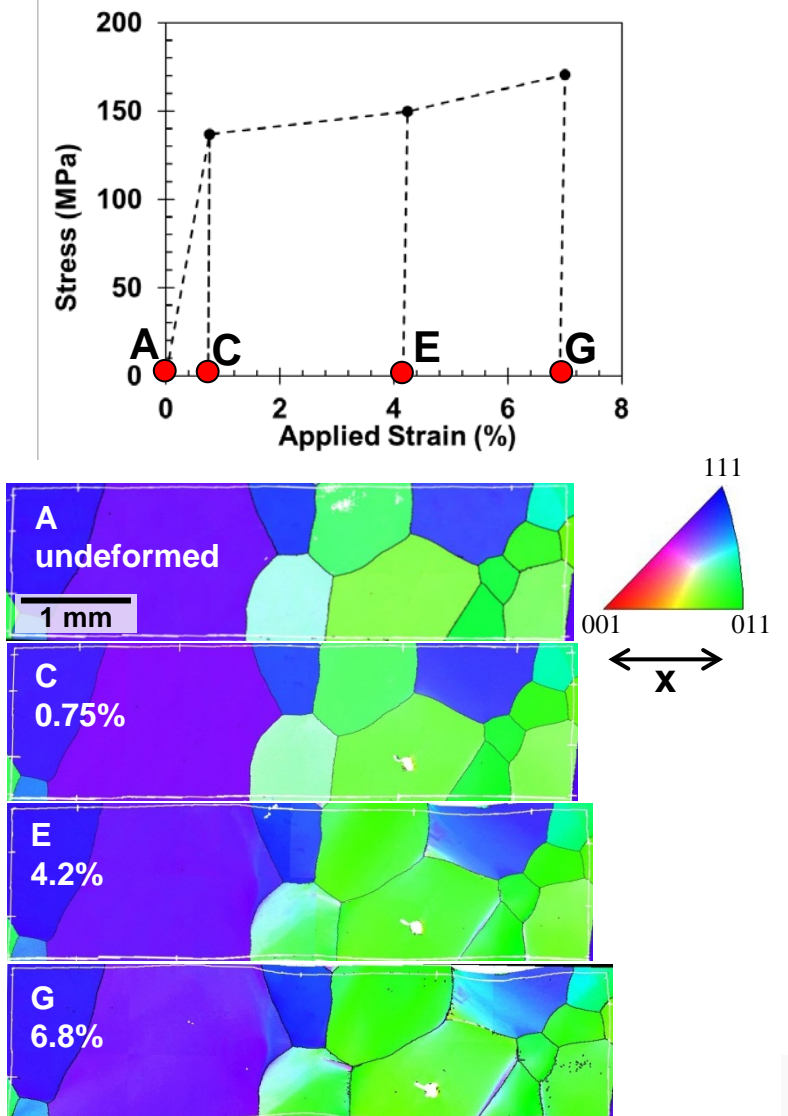


{110} slip

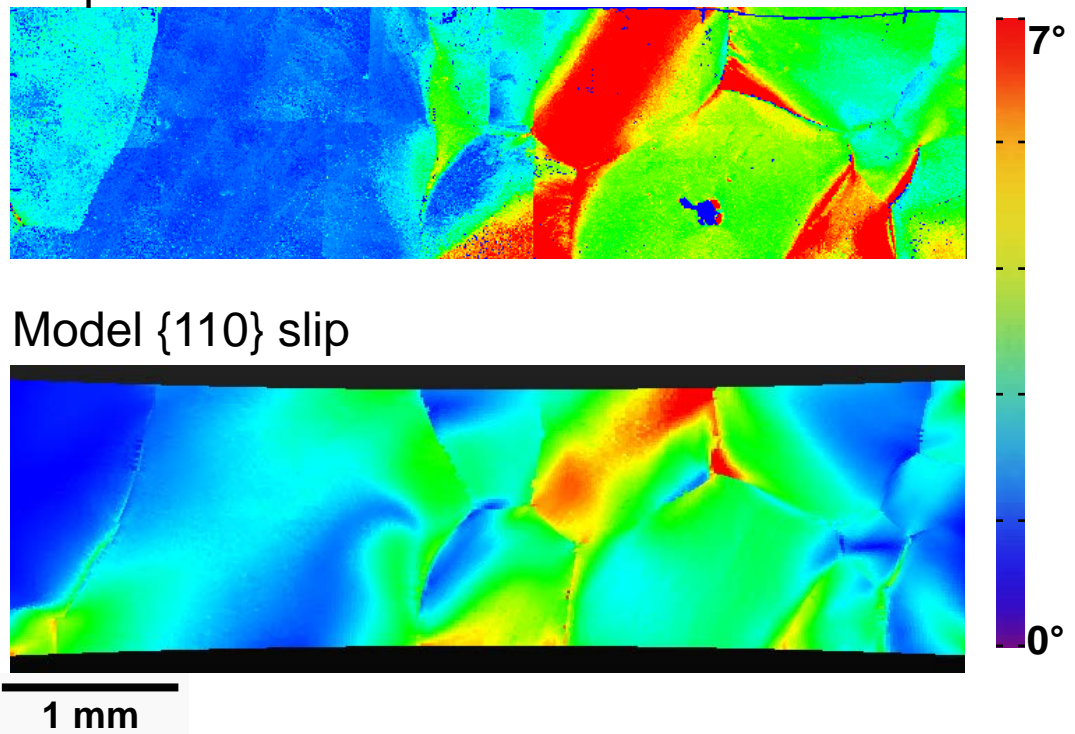
{112} slip

1. **Background**
2. **Experimental setup**
3. **Model details**
4. **Model validation- strain fields**
5. **Model validation- crystal rotations**
6. **Conclusions**

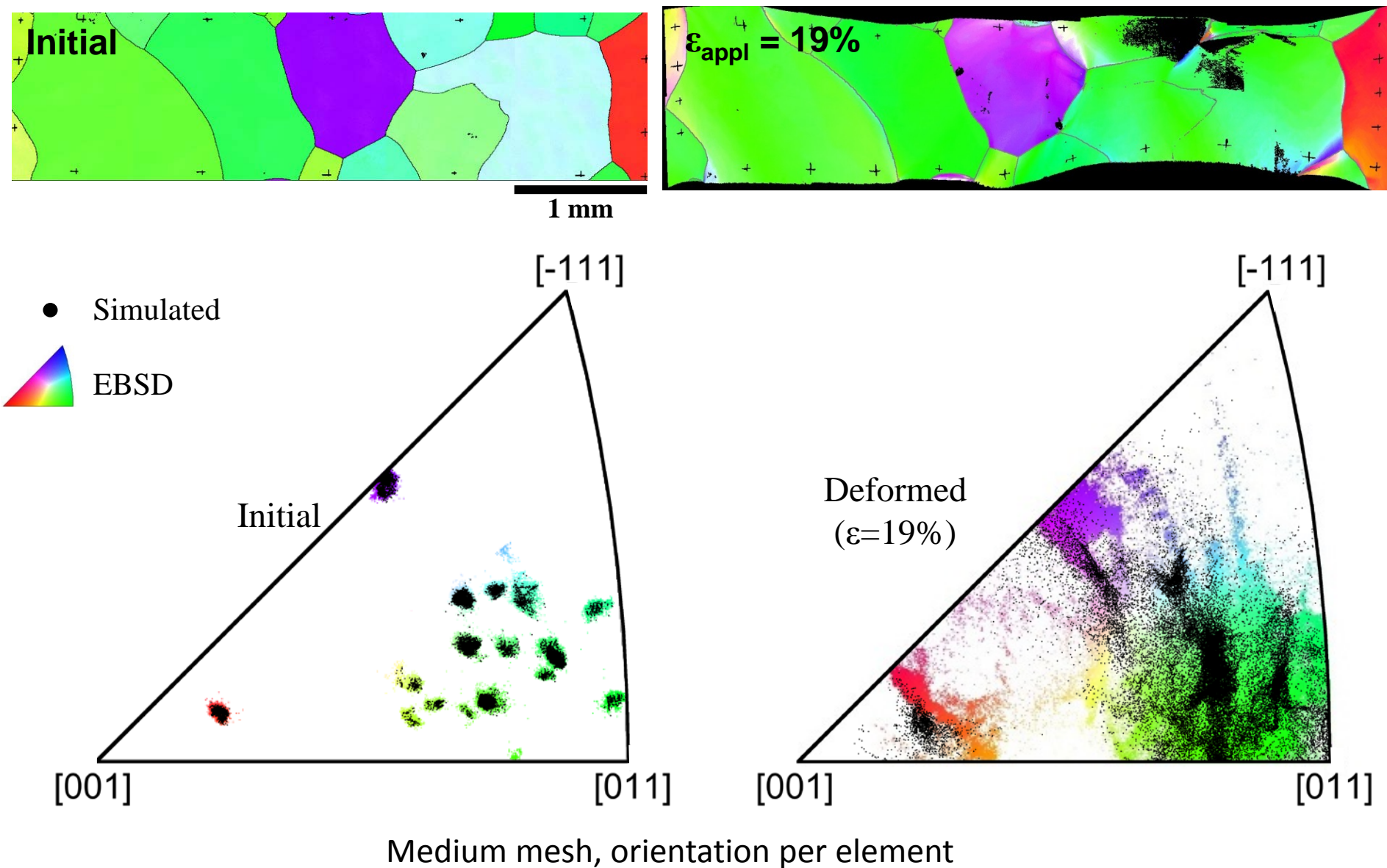
# Oligo 1 grain rotation: model and experiment show good qualitative agreement.



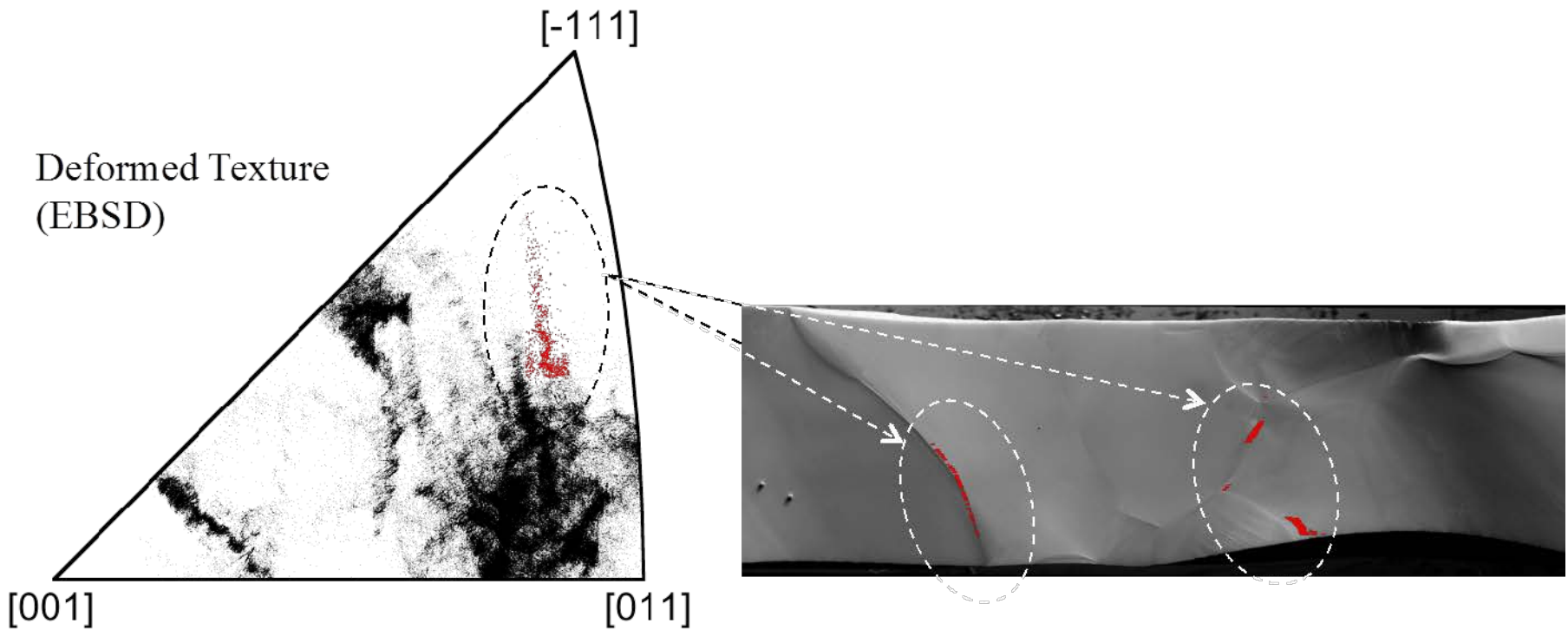
**Grain rotation at 4.2% applied strain**  
Experiment



# Oligo 2: Compare texture evolution.

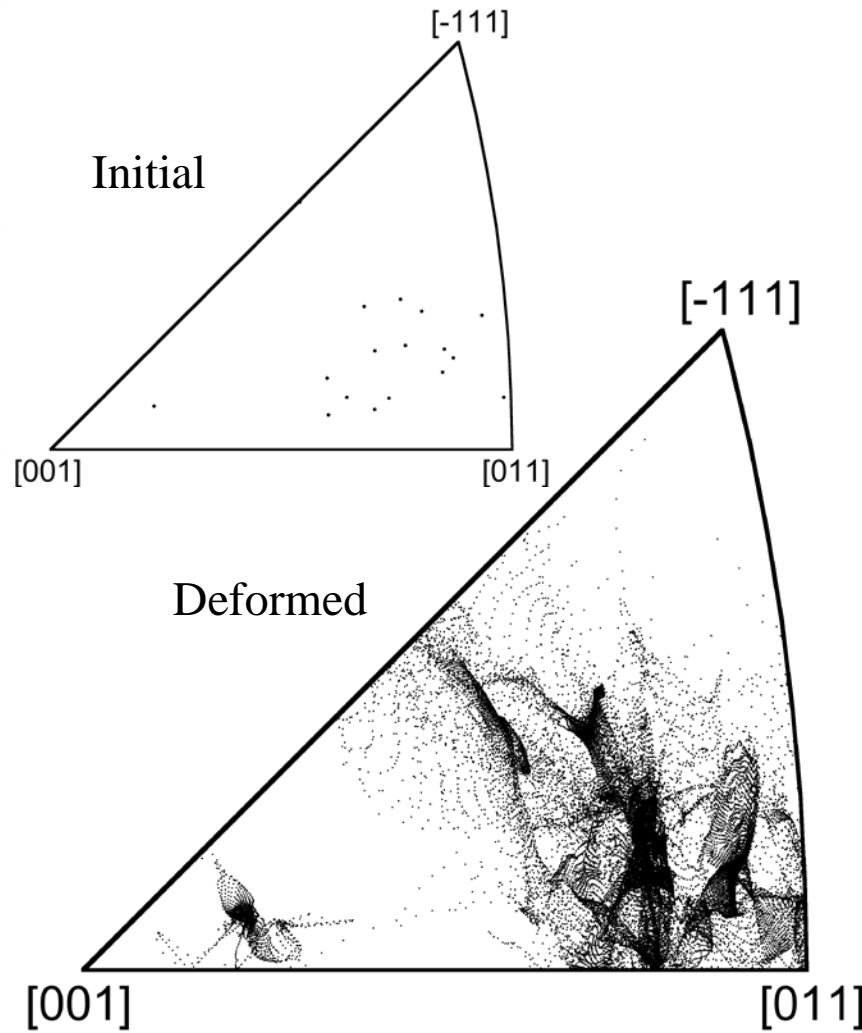


# Streaks in inverse pole figure (from experiment) are at grain boundaries.

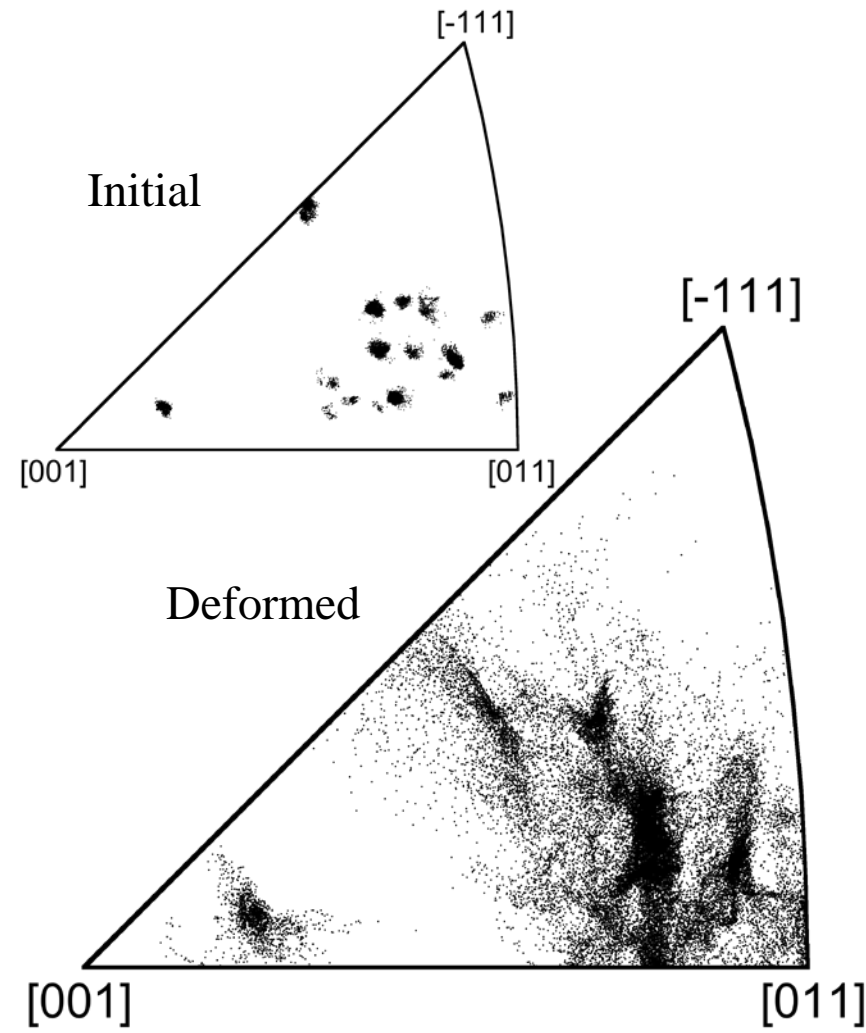


Defining orientations per element (instead of an orientation per grain) gives more realistic inverse pole figures.<sup>34</sup>

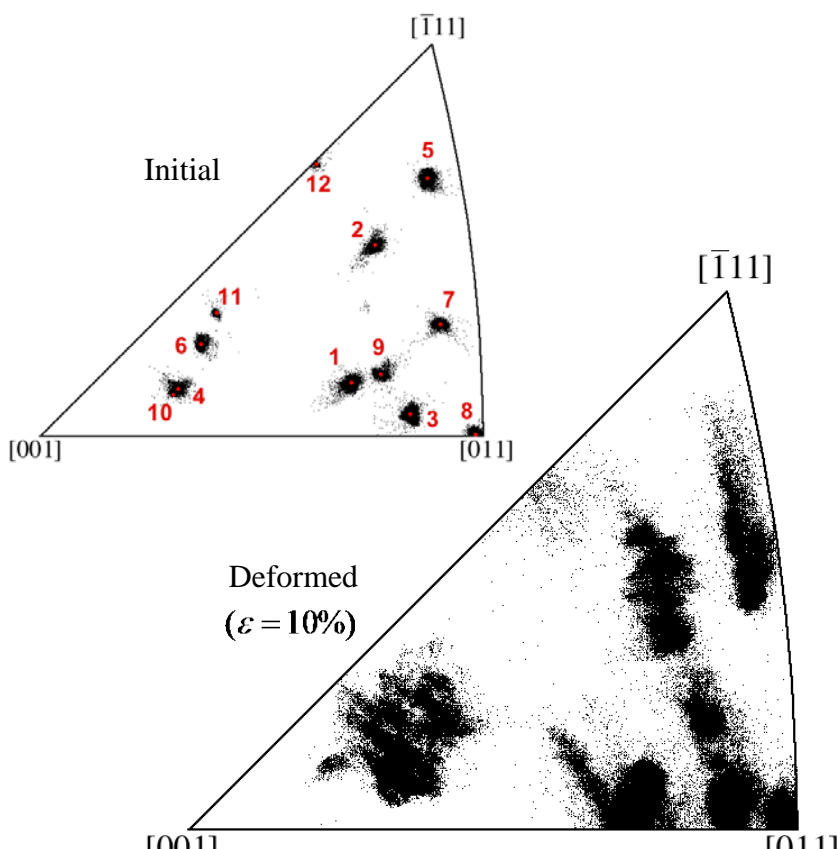
Orientation per grain



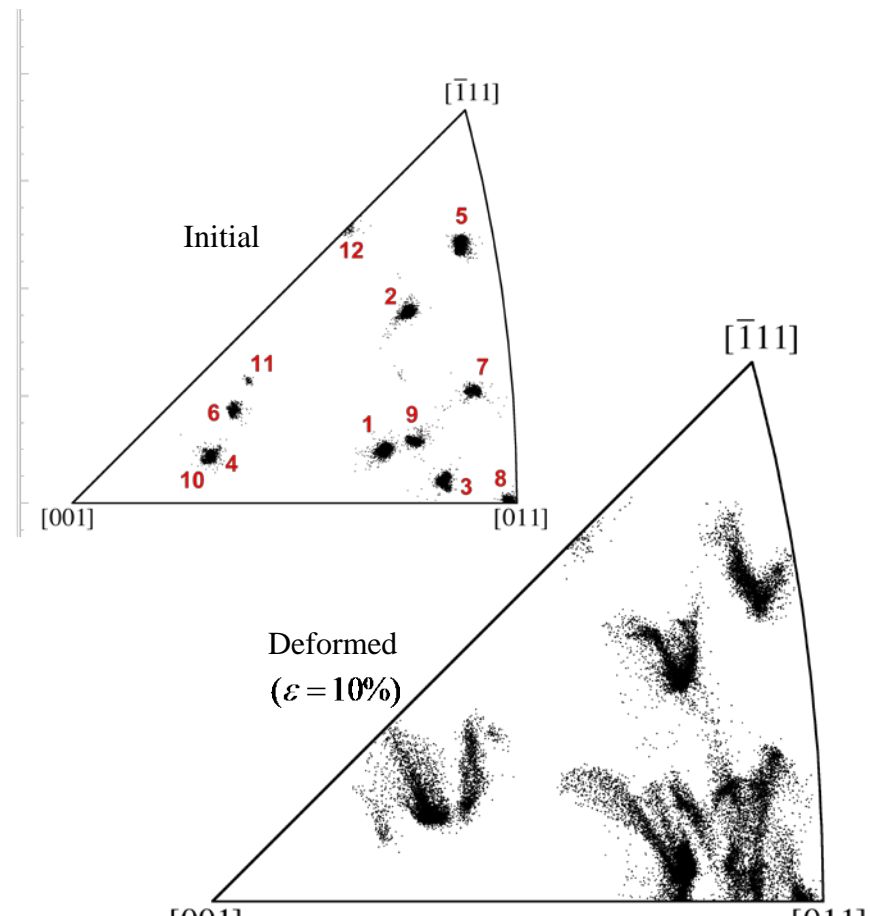
Orientation per element



# Oligo 4: Grain rotations



(a) Measured (EBSD)



(b) Predicted (CP-FEM)

1. **Background**
2. **Experimental setup**
3. **Model details**
4. **Model validation- strain fields**
5. **Model validation- crystal rotations**
6. **Conclusions**

# Conclusions

37

- **Strain predictions show good agreement with experiments.**
  - Quantitative pointwise agreement within ~3% strain.
  - Results affected by 3d issues
  - Fracture initiation observed at location of highest predicted strain.
- **Grain rotations are more challenging.**
  - Improved grain boundary modeling has promise.
- **Effects of model parameters**
  - Still unclear whether {110} or {112} (or combination) is better.
  - Pseudo 3D model is much more accurate than 2D.
  - Defining orientations element-wise makes grain rotations look more realistic.

